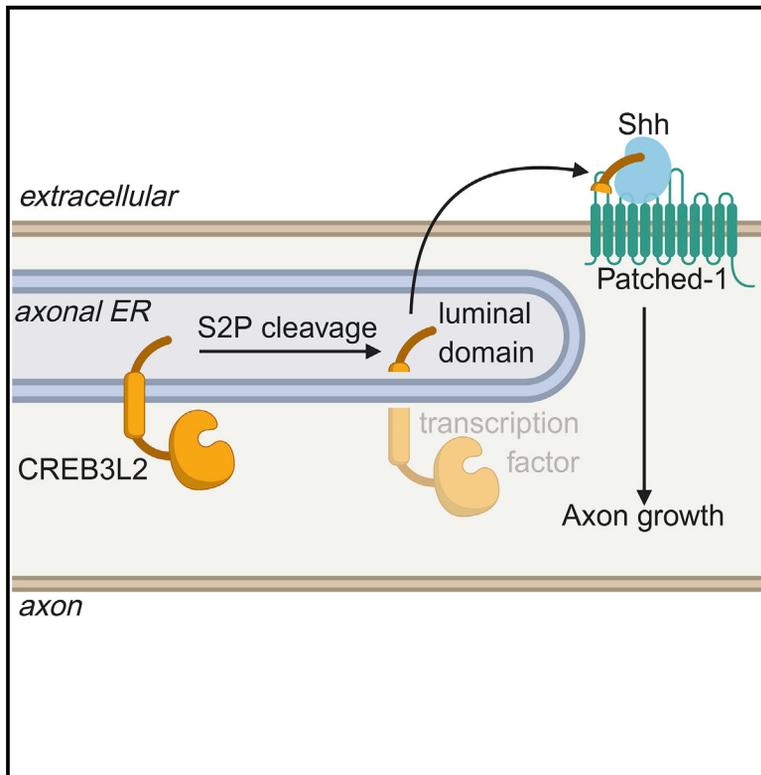Article

Promotion of Axon Growth by the Secreted End of a Transcription Factor

Graphical Abstract

Authors

Ethan P. McCurdy, Kyung Min Chung,
Carlos R. Benitez-Agosto, Ulrich Hengst

Correspondence

uh2112@cumc.columbia.edu

In Brief

McCurdy et al. describe a cell-autonomous mechanism by which developing axons promote their own growth. They show that the ER stress-related protease S2P cleaves the transcription factor CREB3L2, liberating its C terminus. The C terminus of CREB3L2 promotes sonic hedgehog signaling in developing axons, leading to enhanced axon growth.

Highlights

- Site 2 protease (S2P) is localized to developing axons and required for axon growth

- S2P cleaves the transcription factor CREB3L2, an ER stress transducer, in axons

- The C terminus of CREB3L2 is secreted and required for normal axon growth

- Secreted C-terminal CREB3L2 enhances Shh binding to Patched-1 along sensory axons

CellPress

Promotion of Axon Growth by the Secreted End of a Transcription Factor

Ethan P. McCurdy,[1] Kyung Min Chung,[2] Carlos R. Benitez-Agosto,[2] and Ulrich Hengst[2,3,4,*]

[1]Integrated Program in Cellular, Molecular and Biomedical Studies, Vagelos College of Physicians and Surgeons, Columbia University, New York, NY 10032, USA
[2]The Taub Institute for Research on Alzheimer's Disease and the Aging Brain, Vagelos College of Physicians and Surgeons, Columbia University, New York, NY 10032, USA
[3]Department of Pathology and Cell Biology, Vagelos College of Physicians and Surgeons, Columbia University, New York, NY 10032, USA
[4]Lead Contact
*Correspondence: uh2112@cumc.columbia.edu
https://doi.org/10.1016/j.celrep.2019.08.101

SUMMARY

Axon growth is regulated externally by attractive and repulsive cues generated in the environment. In addition, intrinsic pathways govern axon development, although the extent to which axons themselves can influence their own growth is unknown. We find that dorsal root ganglion (DRG) axons secrete a factor supporting axon growth and identify it as the C terminus of the ER stress-induced transcription factor CREB3L2, which is generated by site 2 protease (S2P) cleavage in sensory neurons. S2P and CREB3L2 knockdown or inhibition of axonal S2P interfere with the growth of axons, and C-terminal CREB3L2 is sufficient to rescue these effects. C-terminal CREB3L2 forms a complex with Shh and stabilizes its association with the Patched-1 receptor on developing axons. Our results reveal a neuron-intrinsic pathway downstream of S2P that promotes axon growth.

INTRODUCTION

During neural development, numerous extracellular guidance and neurotropic cues steer and modulate axon growth (Stoeckli, 2018). In addition to these extrinsic signals, there are also neuron-intrinsic pathways that regulate axon growth. These pathways are essential because they allow axons to carry out diverse behaviors in response to a limited number of extracellular signaling factors. For example, differential expression of transcription factors determines responsiveness to guidance cues, and these factors can act as retrograde signals to relay the information from extrinsic signals from axons to the cell bodies (Butler and Tear, 2007; Polleux et al., 2007).

Transcription factors can be activated in axons by local synthesis (Baleriola et al., 2014; Ben-Yaakov et al., 2012; Cox et al., 2008; Ji and Jaffrey, 2012; Ying et al., 2014) or through intramembrane proteolysis of precursor proteins catalyzed by specific membrane-bound proteases (Hoppe et al., 2001). For example, site 2 protease (S2P) cleaves endoplasmic reticulum

(ER) membrane-bound proteins, leading to generation of soluble cytoplasmic transcription factors (Rawson, 2013). As an organelle, the ER is essential for maintaining cellular homeostasis. In response to various cellular stressors, adaptive response pathways of the unfolded protein response (UPR) are activated in the ER that trigger intracellular changes aimed at preventing cellular damage. Additionally, there is a growing body of evidence that ER stress and the UPR have beneficial or protective neuronal roles aside from reacting to acute stressors.

Examples for this so-called physiological ER stress in the nervous system include regulation of memory formation (Martínez et al., 2016), dendrite morphogenesis (Wei et al., 2015), and regenerative axon growth (Ohtake et al., 2018; Oñate et al., 2016; Ying et al., 2015). The best-known UPR pathways are those mediated by PERK, IRE1, and ATF6. More recently, another group of transmembrane ER stress transducers has been identified, collectively called the OASIS family (Asada et al., 2011). The N-terminal cytoplasmic domains of OASIS family members comprise basic leucine zipper domain (bZIP) transcription factors, and cleavage by site 1 protease (S1P) and/or S2P releases the transcriptionally active end. OASIS proteins are activated in response to very mild physiological ER stress, meaning that they are necessary for regulation of their target genes under physiological conditions (Kondo et al., 2007, 2011).

Here we asked whether S2P-dependent activation of transcription factors within axons is required for generation of retrograde signals from axons to cell bodies during axonal development. We found that axonal S2P activity is required for axon growth; surprisingly, not via regulation of transcription but, instead, by liberating a secreted peptide derived from the C terminus of the transcription factor CREB3L2. The secreted C-terminal part of CREB3L2 is part of a neuron-intrinsic pathway that supports axon growth by enabling sonic hedgehog (Shh) signaling in developing axons.

RESULTS

S2P Is Required for the Normal Growth of Developing Axons

The presence and activation of transcription factors from the OASIS family in axons (Ying et al., 2014) raised questions of
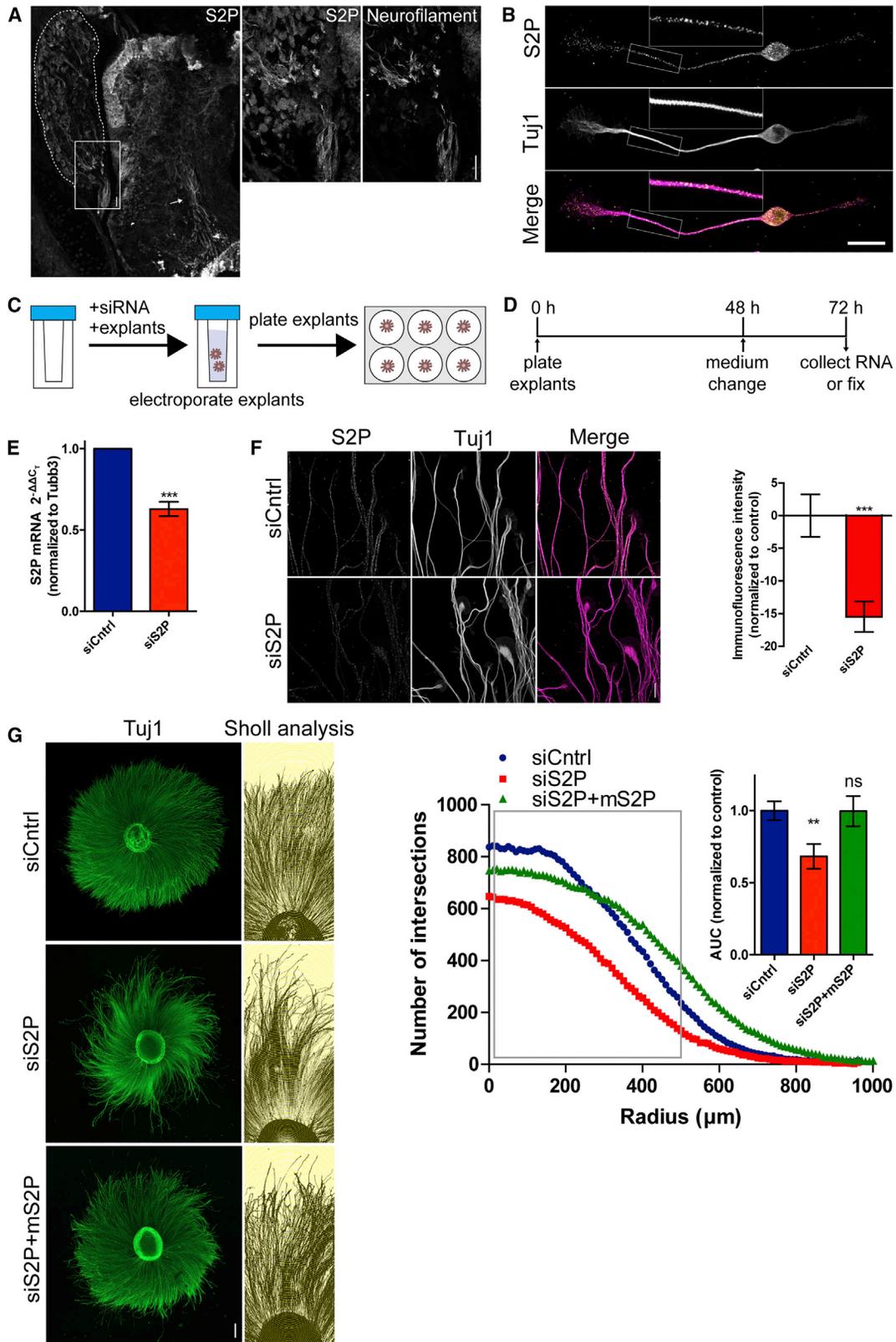
whether S2P is present or active in axons. To address the first of these questions, we stained sections of dorsal root ganglia (DRGs) with adjacent spinal cords of rat embryos for S2P and neurofilament (Figure 1A). We also prepared dissociated embryonic DRG neurons, which were grown for 3 days in vitro (DIV) and labeled with S2P and Tuj1 (Figure 1B). In both types of immunolabeling, a signal for S2P was readily apparent throughout the neuron, including the axon. The prominent expression of S2P in developing axons suggested that it might have a physiological function in axon growth. To test whether S2P is required for axon growth, we suppressed its expression in DRG explants by delivering small interfering RNA (siRNA) with electroporation (Figure 1C). Because DRG explants are comprised of many sensory neurons, they provide a robust approach to assess changes in growth across numerous axons. Following electroporation, the DRG explants were grown in culture for 3 DIV with minimal experimental intervention (Figure 1D). qRT-PCR revealed that electroporation of siRNA targeting S2P efficiently knocked down S2P transcripts in explants compared with a control non-targeting siRNA (Figure 1E). Knockdown of S2P levels in axons was confirmed by quantitative immunofluorescence (Figures 1F and S1A). Explants that received control siRNA exhibited a typical morphology of a fairly round and even halo of axons emanating from the explants. In contrast, S2P siRNA (siS2P)-transfected explants displayed overall shorter axon growth and a more uneven appearance (Figure 1G). To quantitatively assess changes in axon growth, we performed a Sholl analysis of these explants (Ferreira et al., 2014). This analysis revealed a significant reduction in the growth of the axons emanating from siS2P-transfected explants, which was prevented by expression of an siRNA-resistant S2P construct (Figure 1G). Given its prominent localization to axons, we next asked whether S2P activity specifically within axons is required for their development.

Axonal S2P Activity Is Required for Axon Outgrowth

To investigate a potential local role of S2P in outgrowth, we cultured DRGs in microfluidic devices, which allow fluidic isolation of axons and cell bodies (Figure 2A; Hengst et al., 2009; Taylor et al., 2005). In these chambers, three compartments are separated by 500-μm-long microgrooves through which only

axons can extend. We seeded dissociated DRG neurons in an upper compartment and transfected them with control siRNA or siRNA targeting S2P for 48 h (Figure 2B), leading to a significant reduction of S2P expression in axons, as assessed by immunofluorescence (IF) (Figure 2C). Suppression of S2P expression did not interfere with cell viability, as assessed by terminal deoxynucleotidyl transferase dUTP nick end labeling (TUNEL) assay (Figure 2D). To assess axon outgrowth, we imaged fields in the most distal compartment before applying fresh medium locally and returning the devices to the incubator. 1 h later, we identified the same fields and measured how much individual axons had grown. The rate of axon outgrowth was significantly reduced upon delivery of S2P siRNA compared with control axons (Figure 2E). Next, to test the role of axonally localized S2P, we applied the S2P inhibitor nelfinavir (NF) specifically to axons during the growth assay (Guan et al., 2011, 2012, 2015). We observed that the rate of axon outgrowth was diminished when NF was acutely applied in the distal axonal compartment of microfluidics for 1 h (Figure 2F). Together, these results demonstrated that suppression of S2P activity within axons impairs axon growth rates. To identify what acts downstream of S2P activity, we next considered the possibility that S2P activates a retrograde-acting transcriptional signal, such as a transcription factor, in the axon.

Intra-axonal S2P Promotes Growth Locally

S2P is a known regulator of the SREBP family of transcription factors that control the expression of genes required for fatty acid metabolism. Therefore, we considered that S2P inhibition or knockdown could interfere with lipid synthesis, required for expansion of the plasma membrane of developing axons (Pfenninger, 2009). To test this idea, we electroporated DRG explants with control or S2P siRNA for 72 h and determined the mRNA levels by qRT-PCR for two major transcriptional targets of SREBPs, fatty acid synthase (FAS) and 3-hydroxy-3-methylglutaryl-coenzyme A (HMG-CoA) reductase (Brown and Goldstein, 1997; Horton et al., 2003; Figure 3A). Contrary to expectation, knockdown of S2P did not have an effect on the mRNA levels of either transcript, as measured by qRT-PCR (Figure 3B). This observation led us to reconsider the hypothesis that axonal

---

Figure 1. Axonal S2P Is Required for Axon Growth

(A) Immunohistochemistry for S2P on a DRG and spinal cord of an embryonic day 16 (E16) rat embryo. The 10X panel is labeled with neurofilament, and the arrow points to axons of spinal cord neurons. The DRG is outlined with a dotted line. The 40X panel shows the staining for neurofilament and S2P, which is expressed in the nerve bundle exiting the DRG. Scale bar, 25 μm.

(B) Rat embryonic DRG neurons were seeded at a low density, cultured for 3 DIV, and stained for S2P and tubulin. Center panel focuses on the respective areas outlined with a rectangle. Scale bar, 20 μm.

(C) Electroporation. DRG explants were dissected from E14 rat embryos and transferred to a cuvette containing electroporation buffer and control or targeting siRNA. Following electroporation, individual explants were plated in culture dishes.

(D) Experimental design for (E)–(G). Explants were plated on DIV 0 and cultured for 48 h. On DIV 2, the medium was completely exchanged with fresh DRG growth medium containing 5 ng mL^{-1} NGF, and either total RNA was collected or explants were fixed on DIV 3.

(E) DRG explants were electroporated with non-targeting control siRNA or siRNA targeting S2P and cultured for 3 DIV. S2P mRNA levels were quantified by RT-PCR in lysates obtained from the explants 72 h after electroporation. Means ± SEM (n = 5 biological replicates). Wilcoxon signed-rank test, ***p $\leq$ 0.001.

(F) DRG explants were electroporated with non-targeting control siRNA or siRNA targeting S2P and cultured for 3 DIV. Axonal S2P levels were measured by IF. Percent KD relative to control is shown. Means ± SEM, 10–15 optical fields per condition (n = 3 biological replicates). Mann-Whitney t test, ***p $\leq$ 0.001. Scale bar, 20 μm.

(G) DRG explants were electroporated and cultured as described in (C) and (D). Explants were fixed and visualized by IF staining against Tuj1, and axon growth was assessed using the Sholl analysis. The area under the curve (AUC) was measured between conditions. Means ± SEM of 2–7 explants per condition (n = 3–5 biological replicates). Kruskal-Wallis tests with Dunn's multiple comparisons tests, **p $\leq$ 0.01; ns, not significant. Scale bar, 250 μm.
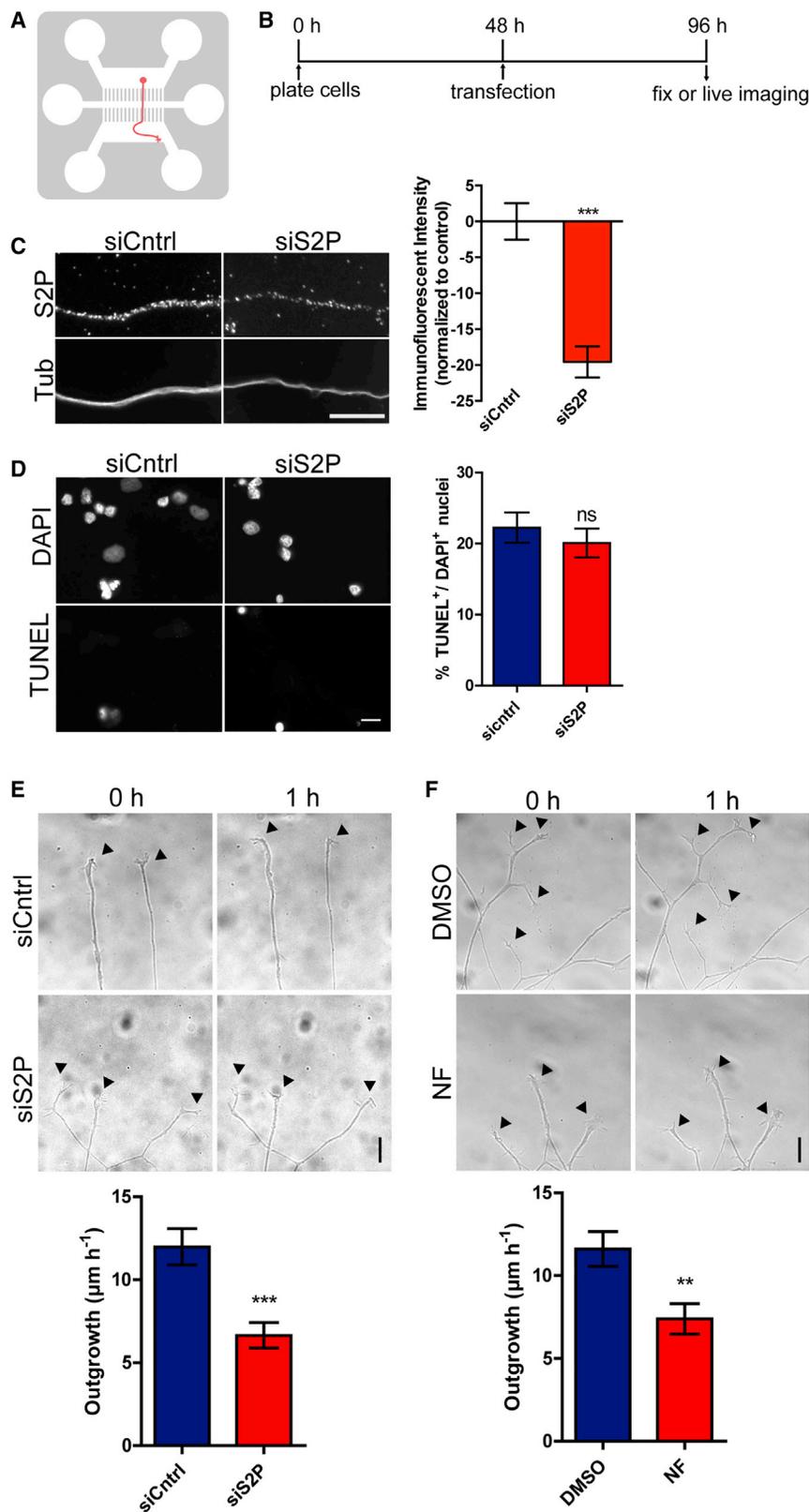
See also Figure S1.

Figure 2. Axonal S2P Activity Promotes Axon Growth

(A) Depiction of a microfluidics device used to isolate axons. DRG neurons were seeded in the top (somatic) compartment and cultured as described in (B). Live-cell microscopy was performed in the bottom (most distal) axonal compartment.

(B) Experimental design for (C)–(F). DRG neurons were seeded in microfluidics and cultured for 2 DIV, at which point the medium was completely exchanged for DRG growth medium containing 5 ng mL^{-1} NGF, and non-targeting control siRNA or siRNA targeting S2P was transfected into all compartments when applicable. 48 h later, DRGs were prepared for IF (C) or TUNEL (D) or used for live-cell microscopy.

(C) DRG neurons were cultured and treated as in (A) and (B). Axonal S2P levels were measured by IF. Percent KD relative to control is shown. Means ± SEM of 10–15 optical fields per condition (n = 4 biological replicates). Mann-Whitney t test, ***p ≤ 0.001. Scale bar, 10 μm.

(D) Neurons were cultured and treated with siRNA as in (A) and (B). Cell death was assessed by TUNEL assay. Means ± SEM of 10–20 optical fields per condition (n = 3 biological replicates). Mann-Whitney t test; ns, not significant. Scale bar, 15 μm.

(E) Axon growth between siCntrl and siS2P was measured by comparing images taken before and after axonal application of fresh medium for 1 h. Means ± SEM of 10–20 fields per condition, 126 siCntrl axons and 121 siS2P axons total (n = 4 biological replicates). Mann-Whitney t test, ***p ≤ 0.001. Scale bar, 20 μm.

(F) Axon growth between DMSO and NF was measured by comparing images taken before and after axonal application of fresh medium in the most distal axonal compartment containing either DMSO or NF (15 μM) for 1 h. Means ± SEM of 10–20 fields per condition, 110 DMSO-treated and 92 NF-treated axons total (n = 4 biological replicates). Mann-Whitney t test, **p ≤ 0.01. Scale bar, 20 μm.
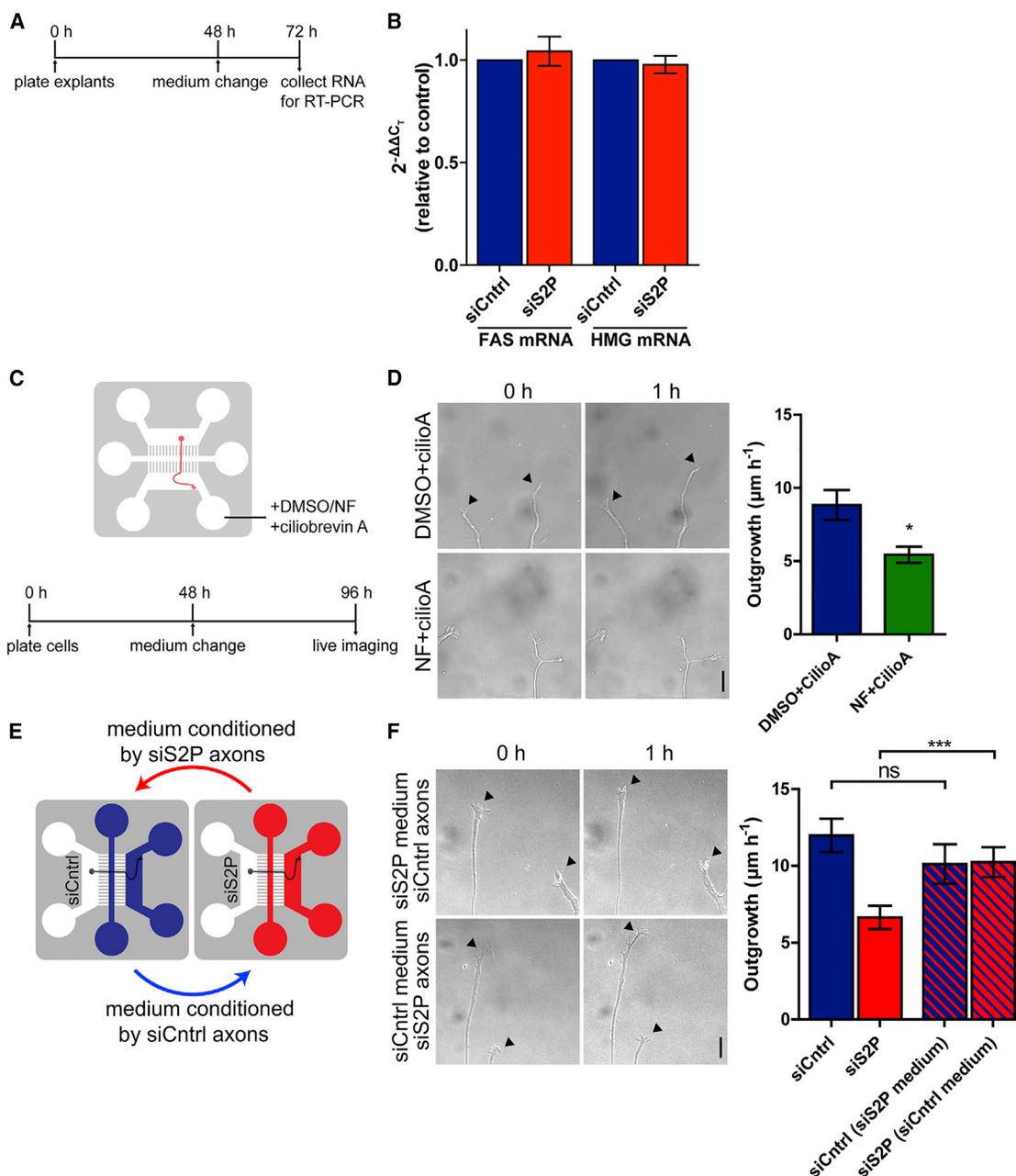
Figure 3. Axonal S2P Acts through a Secreted Factor

(A) Experimental design for (B). DRG explants were electroporated with non-targeting control siRNA or siRNA targeting S2P and cultured for 3 DIV. RNA was collected at 72 h, and RT-PCR was performed to assess efficiency of KD.

(B) Fatty acid synthase (FAS) and HMG-CoA reductase mRNA levels were quantified by qRT-PCR in lysates obtained from the explants 72 h after electroporation. Means ± SEM (n = 3–4 biological replicates). Mann-Whitney t tests, no significant differences.

(C) Experimental design for (D). DRG neurons were seeded in microfluidics and cultured for 96 h. Axons in the distal compartment were treated with DMSO and NF concomitant with 30 μM ciliobrevin A for 1 h and live-imaged in the same compartment.

(D) Axon outgrowth assay of DRG neurons treated with DMSO or NF (15 μM) with ciliobrevin A (30 μM). Means ± SEM of 10–20 fields per condition, 93 DMSO-treated and 122 NF-treated axons total (n = 3 biological replicates). Mann-Whitney t test, *p ≤ 0.05. Scale bar, 20 μm.

(E) Representation of the axonal medium exchange experiment. DRG neurons were cultured and transfected with siRNA as described earlier. On DIV 4, axonal medium was replaced with fresh medium for 6 h. Images of initial fields of each condition were then collected, axonal media from control and S2P-targeting siRNA were exchanged, and images were acquired 1 h later to measure outgrowth.

(F) Axon growth measurement of DRG neurons cultured as described in (E). The siCntrl and siS2P data are from Figure 2D and shown here for comparison. Means ± SEM of 10–20 fields per condition, 95 siCntrl and 89 siS2P axons total (n = 4 biological replicates). Kruskal-Wallis test with Dunn's multiple comparisons test, **p ≤ 0.01. Scale bar, 20 μm.
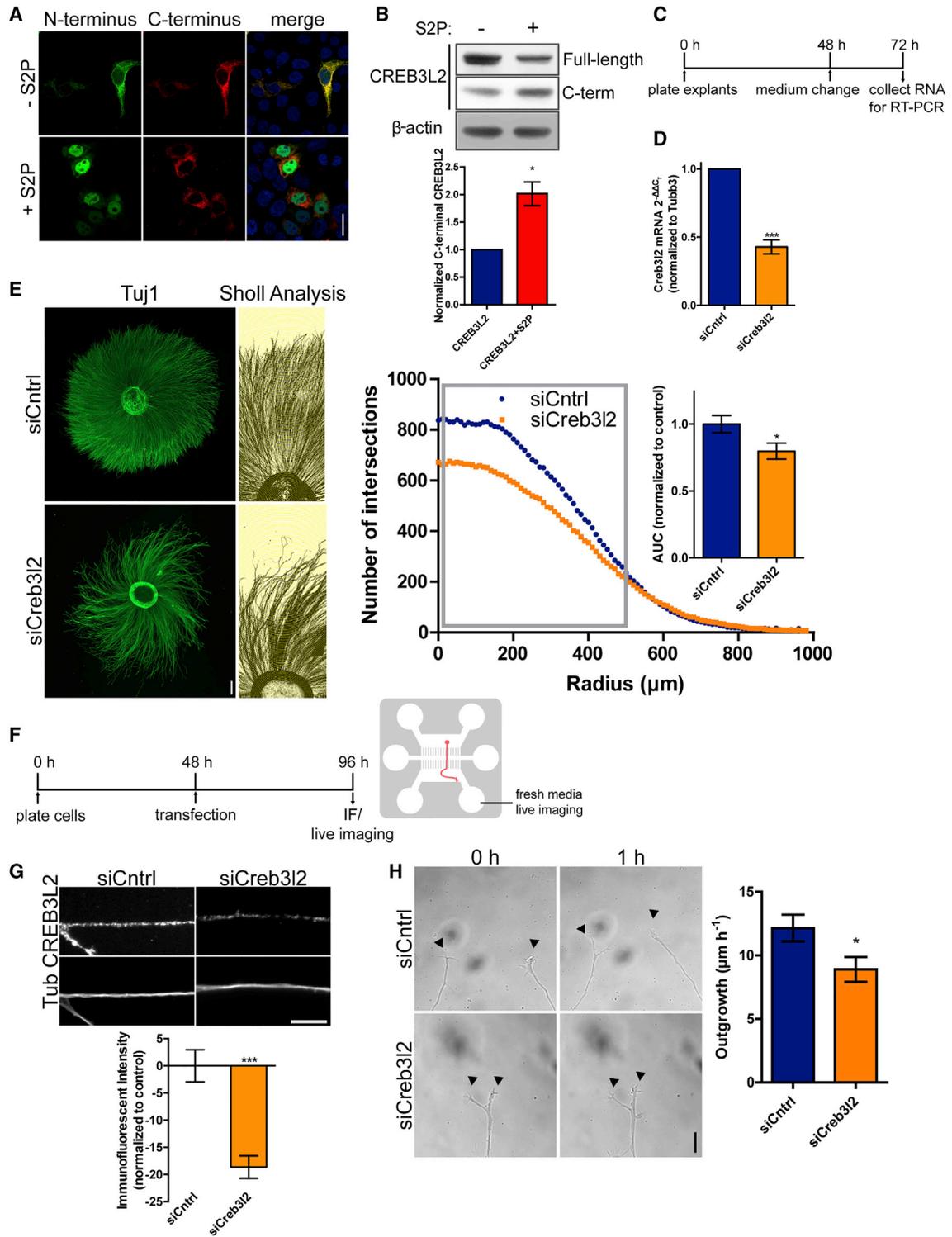
Figure 4. CREB3L2 Is Required for Axon Growth

(A) HEK293T cells were grown and transfected with constructs expressing S2P with or without CREB3L2 fused to GFP on the N terminus and mCherry or FLAG on the C terminus. Representative images are shown from 3 independent replicates. Scale bar, 20 μm.

(B) Western blot of HEK293T cells overexpressing a CREB3L2 fusion protein with or without S2P. Immunoblotting was performed for full-length and C-terminal CREB3L2 fragments and a loading control (top). Production of the CREB3L2 C terminus by S2P was quantified in FIJI (bottom). A representative blot is shown. Means ± SEM of 3 independent replicates. Paired t test, *p ≤ 0.05.

(legend continued on next page)

S2P is required for the generation of a retrograde signal, such as a transcription factor. In our live growth assays performed in microfluidic devices, the distance from growth cones to their somata is at minimum 1,500 μm, given the separation of the compartments by the microgrooves. Assuming the maximum speed of cytoplasmic dynein and kinesin-3, the fastest antero-grade member of the kinesin family, the 1-h assay would not allow a signal to reach the soma and the response to return to growth cones with enough time to significantly affect axon growth (Twelvetrees et al., 2016). Our findings instead suggest that S2P exerts an effect on outgrowth by acting through a local intra-axonal mechanism. To directly test the requirement for a signal to reach the cell body from the distal axon, we inhibited dynein-dependent retrograde transport in axons by co-treating axons with NF and ciliobrevin A (Firestone et al., 2012; Figure 3C). Because all motor-based retrograde transport in axons is mediated by dynein, we reasoned that if S2P acts in the same pathway as dynein by generating a retrograde transcription factor, then the corresponding decrease in outgrowth resulting from S2P inhibition would be prevented in the presence of ciliobrevin A. The effective concentration of ciliobrevin A that we used in microfluidics (30 μM) was established previously (Baleriola et al., 2014). We found that, even in the presence of ciliobrevin A, axon outgrowth was diminished by NF, suggesting that S2P inhibition prevents a local growth-promoting response from occurring rather than acting through a retrograde signal (Figure 3D).

Previous studies have reported that DRG axons may secrete proteins (González et al., 2016; Merianda and Twiss, 2013; Merianda et al., 2009). Hence, one explanation for diminished outgrowth under S2P knockdown or inhibition is that S2P generates a locally secreted factor that promotes axon growth in an auto- or paracrine manner. To test whether S2P is required for generation of a growth-promoting secreted factor, we exchanged the axonal medium of control and S2P knockdown DRGs (Figure 3E) and measured axon growth over 1 h as before. The impaired outgrowth of DRG axons with S2P knockdown (KD) was rescued by the application of medium from control axons (Figure 3F). Notably, the rescue in outgrowth was due to an increase in axon growth for siS2P neurons that received the control medium. This result suggests that control axons locally produce a secreted factor in the medium that the S2P-deficient axons can no longer generate. Together, these results reveal

that S2P acts locally by generating a secreted factor that regulates axon outgrowth.

Loss of CREB3L2 Phenocopies S2P Inhibition and KD

Previous work in chondrocytes revealed that cleavage by S2P in some cases (OASIS, CREB3L2, and CREB4) generates not only one but two bioactive proteins: the transcription factor in the cytoplasm and the C-terminal part in the ER lumen (Saito et al., 2014). These luminal domains are secreted, and at least one of them, the luminal portion of CREB3L2, acts in an auto- or paracrine manner as a growth-promoting factor on chondrocytes (Saito et al., 2014). Several publications have proposed that CREB3L2 is cleaved not only by S2P but also by S1P (Kondo et al., 2007; Saito et al., 2014). This assumption is primarily based on analogies with ATF6 and SREBP (Shen and Prywes, 2004), but, importantly, cleavage of CREB3L2 by S2P occurs in the presence of brefeldin A (i.e., without being transported to the Golgi) and with the S1P cleavage site mutated (Kondo et al., 2007). First, to directly test whether S2P activity is sufficient to drive CREB3L2 cleavage, we expressed S2P together with CREB3L2 fused to GFP on its N-terminal, transcriptionally active portion and fused to mCherry on its C terminus in HEK293 cells. In the absence of S2P, the majority of the GFP and mCherry signals overlap in a perinuclear, ER-like pattern (Figure 4A). Upon co-expression of S2P, the majority of the GFP signal (i.e., the transcription factor part of CREB3L2) translocated to the nucleus, whereas the mCherry signal remained perinuclear. In parallel, we found, by immunoblot, that S2P expression drove the production of the CREB3L2 C terminus (Figure 4B). Together, these results demonstrate that S2P alone is sufficient to cleave CREB3L2 and generate its C terminus, as indicated previously (Kondo et al., 2007).

Given that the C terminus of CREB3L2 can act as a growth factor, we next asked whether depleting available C-terminal CREB3L2 by knocking down CREB3L2 would phenocopy the axonal growth defects seen in S2P-deficient neurons. Electroporation of DRG explants for 72 h significantly reduced the levels of CREB3L2 mRNA (Figures 4C and 4D) and the levels of CREB3L2 protein in axons (Figure S1B), causing an axon growth phenotype reminiscent of what we observed for S2P KD (Figure 4E). Next we examined whether outgrowth of DRG axons was affected by knocking down CREB3L2 in microfluidic chambers (Figures 4F

(C) Experimental design for (D). DRG explants were electroporated with non-targeting control siRNA or siRNA targeting CREB3L2 and cultured for 3 DIV. RNA was collected at 72 h, and RT-PCR was performed to assess efficiency of KD.

(D) CREB3L2 mRNA levels were quantified by qRT-PCR in lysates obtained from the explants 72 h after electroporation with siRNA. Means ± SEM (n = 4 biological replicates). Mann-Whitney t test, ***p ≤ 0.001.

(E) DRG explants were electroporated and cultured as in (C). Explants were fixed, visualized by IF staining against Tuj1, and axon growth was assessed using the Sholl analysis. AUC was measured between conditions. Means ± SEM of 2–7 explants per condition (n = 5 biological replicates). Mann-Whitney t test, *p ≤ 0.05. Scale bar, 250 μm. Because electroporation for siCntrl, siS2P, and siCreb3l2 was performed in parallel, the same representative siCntrl explant image (Figure 1G) is shown for reference.

(F) Experimental design for (G) and (H). DRG neurons were cultured in microfluidics for 2 DIV, and non-targeting control siRNA or siRNA targeting CREB3L2 was transfected into all compartments for 48 h. On DIV 4, the DRGs were fixed and prepared for IF (G) or live imaging (H).

(G) CREB3L2 levels were measured by quantitative IF to confirm axonal KD. Percent KD relative to control is shown. Means ± SEM of 10–15 optical fields per condition (n = 3 biological replicates). Mann-Whitney t test, ***p ≤ 0.001. Scale bar, 10 μm.

(H) Axon outgrowth assay of DRG neurons cultured and treated as in (F). Axon growth was measured by comparing images taken before and after axonal application of fresh medium for 1 h. Means ± SEM of 10–20 fields per condition, 128 siCntrl and 114 siCreb3l2 axons total (n = 4 biological replicates). Mann-Whitney t test, *p ≤ 0.05. Scale bar, 20 μm.

See also Figure S1.

and 4G). We found that axons of neurons deficient in CREB3L2 had impaired rates of outgrowth compared with control axons (Figure 4H). Together, these results indicate that CREB3L2 can be cleaved in an S2P-dependent manner and that knocking down CREB3L2 phenocopies KD or inhibition of S2P, suggesting that the luminal domain of CREB3L2 might be an S2P-dependent, secreted, growth-promoting factor in neurons.

S2P Generates C-Terminal CREB3L2 in DRG Neurons

To investigate whether S2P generates the C terminus of CREB3L2 in axons, we used a proximity ligation assay (PLA) with an antibody pair recognizing the N- and C-terminal parts of the protein, respectively (Figure 5A). DRGs were cultured in microfluidic chambers for 4 DIV, and we applied DMSO or NF to the axonal compartment for 24 h (Figures 5B and 5C). Sparse PLA signals for full-length CREB3L2 were detectable in axons, with a significant increase upon inhibition of S2P with NF (Figure 5D), establishing that CREB3L2 is localized to and processed by S2P within axons. We reasoned that the C terminus of CREB3L2 could be depleted either by preventing generation of the full-length protein or by knocking down CREB3L2 directly using siRNA targeting S2P or CREB3L2, respectively. We confirmed that delivery of S2P or CREB3L2 siRNA significantly reduced endogenous levels of the C-terminal part of CREB3L2 in DRGs (Figure 5E). Next we used an antibody raised against the C-terminal part of CREB3L2 to immunoprecipitate the luminal fragment from the medium of DIV4 DRGs, demonstrating that it is indeed secreted by DRG neurons (Figure 5F). If the C-terminal part of CREB3L2 is the secreted growth-promoting factor, then one might expect to be able to detect it bound to the surface of axons. When we immunostained axons under non-permeabilizing conditions with the antibody raised against the C-terminal part of CREB3L2, we obtained a signal on growth cones and axons that was significantly reduced on axons of neurons deficient in S2P (Figure 5G). Together, these results demonstrate that S2P cleavage of CREB3L2 in DRG axons generates the free C terminus, which is secreted and promotes axon growth and fasciculation in a paracrine manner.

Hedgehog Signaling Is Active in DRGs

In mammalian chondrocytes, the secreted luminal domain of CREB3L2 acts by enhancing Indian hedgehog (Hh) (Ihh) signaling by forming a ternary complex with the Hh receptor Patched-1 and Ihh (Saito et al., 2014). In higher vertebrates, Shh is the principal Hh isoform in neurons, although its signaling mechanism is conserved with Ihh (Pathi et al., 2001). Originally identified as a morphogen, Shh is also an axon guidance cue. Shh attracts pre-crossing spinal cord commissural axons via binding to its receptor Boc and activation of non-canonical, Src family kinase-dependent activation of local translation (Charron et al., 2003; Lepelletier et al., 2017; Okada et al., 2006; Yam et al., 2009). Although DRGs do not respond to exogenously applied Hh, at least adult DRGs express Shh, its receptors, and relevant signaling machinery, including Patched-1 and Smoothened (Martinez et al., 2015; Trousse et al., 2001). Moreover, knocking down Shh in sensory neurons has been shown to impair neuritic growth (Martinez et al., 2015). This suggests that sensory neurons require their own endogenously produced Shh

to grow, which is likely functionally saturating and would explain why they do not respond to exogenous Shh.

Facilitation of Hh signaling by C-terminal CREB3L2 in developing neurons has not been reported previously, prompting us to ask whether this mechanism exists in embryonic DRGs. To test the hypothesis that Shh signaling is required for axon growth of embryonic DRGs, we acutely treated DRG explants with vehicle or robotnikinin, which neutralizes Shh signaling by competitively binding to Shh (Stanton et al., 2009). Under these conditions, we observed that robotnikinin led to a modest reduction in axon growth by Sholl analysis (Figure 6A), suggesting that Shh signaling is required for DRG axonal growth. To see whether depleting the C terminus of CREB3L2 in developing neurons affects the endogenous levels of active Shh, we transfected dissociated DRGs with control, S2P, or CREB3L2 siRNA and tested whole-cell lysates for endogenous Shh 72 h later by immunoblotting. Because the Shh antibody used for immunoblotting specifically recognizes the N terminus, we measured the N-terminal active signaling portion at approximately 19 kDa, which is produced by autocatalysis. KD of S2P or CREB3L2 significantly reduced the amount of active Shh in whole-cell lysates, which includes Shh bound to the cell surface (Figure 6B). An explanation for the decrease in Shh under these conditions is that, without secreted C-terminal CREB3L2, less Shh binds its receptor Patched-1 (Saito et al., 2014). To determine whether the secreted C terminus of CREB3L2 binds to extracellular Shh, we performed co-immunoprecipitation (coIP) on conditioned medium from developing DRGs and detected a complex between the CREB3L2 C terminus and Shh using antibodies against either protein (Figure 6C). To directly investigate whether the C terminus of CREB3L2 actually binds Shh along axons, we electroporated DRG explants with non-targeting control, S2P-targeting, or CREB3L2-targeting siRNA and used a PLA to detect complexes between C-terminal CREB3L2 and Shh after 3 DIV (Figure 6D). Axons deficient in S2P or CREB3L2 had significantly fewer PLA puncta, indicating a reduction in C-terminal CREB3L2-Hh complexes (Figure 6E). Likewise, when we performed PLA for Patched-1 and Shh on equally treated cultures, we observed that fewer ligand-receptor complexes had formed (Figure 6F). The PLA signal was specific because a significant reduction in PLA puncta was observed when one member of each pair was omitted (Figure S2). Together, these results demonstrate that depleting the C terminus of CREB3L2, either by knocking down S2P or CREB3L2 itself, diminishes the ability of neuronally derived Shh to bind Patched-1 along DRG axons.

Exogenous C-Terminal CREB3L2 Rescues Axon Development and Shh Binding to Axons

Finally we asked whether exogenously applied, purified C-terminal CREB3L2 is sufficient to rescue the growth of axons lacking S2P. We cultured explants that were electroporated with control siRNA or siRNA targeting S2P as described above and supplemented the medium with approximately 100 ng ml^{-1} purified C-terminal CREB3L2 (Figures 7A and 7B). Axon growth between control and S2P-deficient axons was indistinguishable, as measured by Sholl analysis (Figures 7C). Importantly, this rescue was not recapitulated by exogenously supplied BSA, which
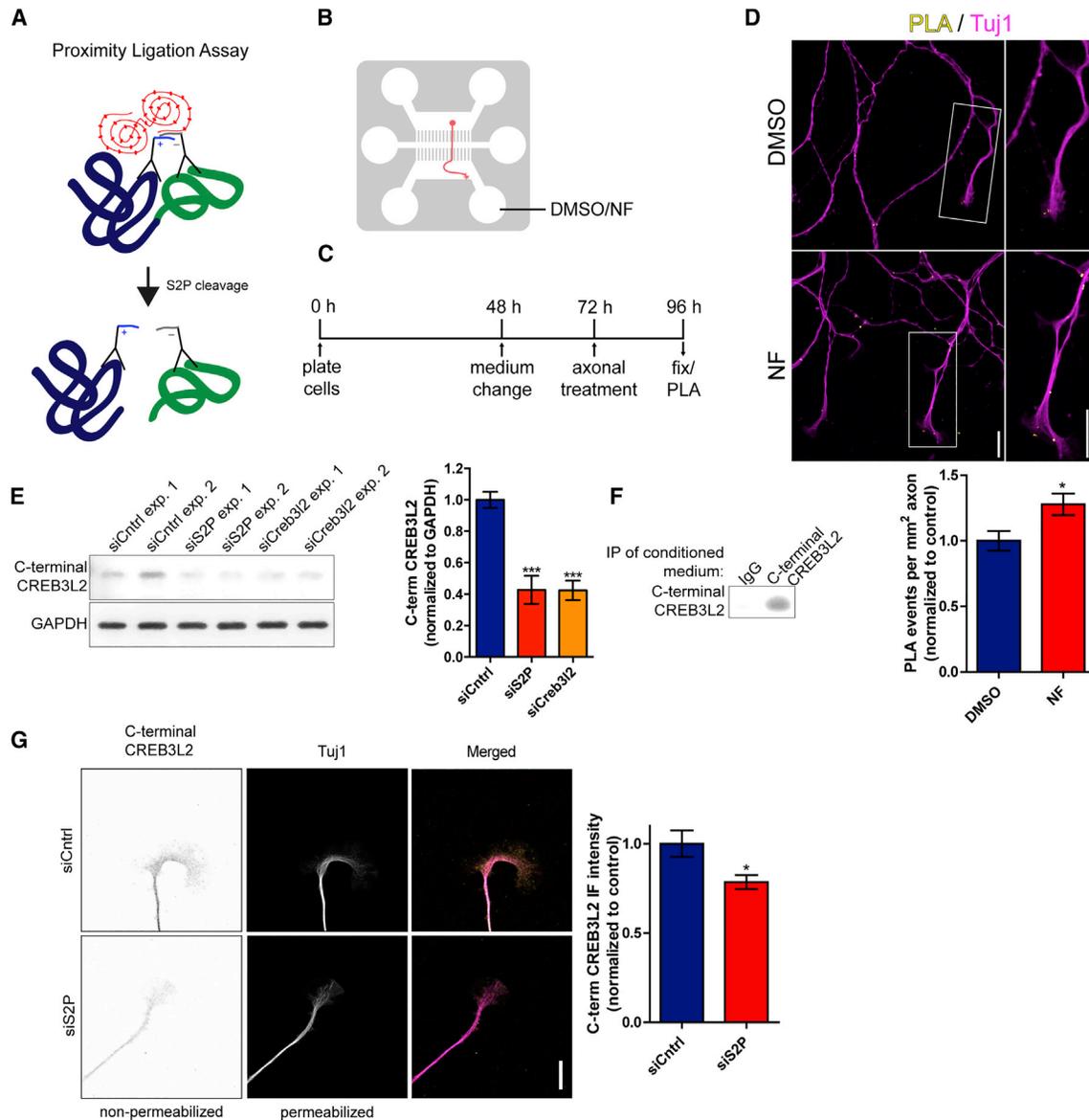
Figure 5. C-Terminal CREB3L2 Is Secreted from Axons in an S2P-Dependent Manner

(A) Principle of the proximity ligation assay. The N- and C termini of CREB3L2 are labeled with antibodies raised in different species and are recognized by positive and negative probes. The CREB3L2 precursor (full-length protein) will not be labeled by the PLA reaction if it has been cleaved by S2P.

(B) Representation of the microfluidics device used in (D) and local treatment with DMSO or NF (15 μM).

(C) DRG neurons were cultured in microfluidics for 3 DIV. Axonal medium was supplemented with DMSO or NF (15 μM) for 24 h. On DIV 4, DRGs were processed for PLA using two antibodies targeting the N or C terminus of CREB3L2.

(D) PLA for full-length CREB3L2 in DRG axons. Means ± SEM of 20–30 optical fields per condition (n = 4 biological replicates). Mann-Whitney t test, *p $\leq$ 0.05. Scale bar, 20 μm.

(E) Dissociated DRGs were cultured for 2 DIV and transfected with non-targeting control siRNA or siRNA targeting S2P or CREB3L2 for 72 h. On DIV 5, whole-cell lysates were obtained and analyzed by western blot for endogenous C-terminal CREB3L2. A blot with 2 repeats is shown. Means ± SEM of 4 biological replicates. Kruskal-Wallis test with Dunn's multiple comparisons test, ***p $\leq$ 0.001.

(F) Immunoprecipitation was performed on conditioned medium of dissociated DRGs using a C-terminal CREB3L2 or immunoglobulin G (IgG) control antibody 48 h after a medium change on DIV 2. A representative IP is shown from 3 independent experiments.

(G) DRG explants were electroporated with non-targeting control siRNA or siRNA targeting S2P and cultured for 3 DIV as described earlier. Explants were fixed and prepared for IF for C-terminal CREB3L2 under non-permeabilizing conditions, followed by permeabilization and staining for Tuj1. Means ± SEM of 10–15 optical fields per condition (n = 3 biological replicates). Mann-Whitney t test, *p $\leq$ 0.05. Scale bar, 10 μm.
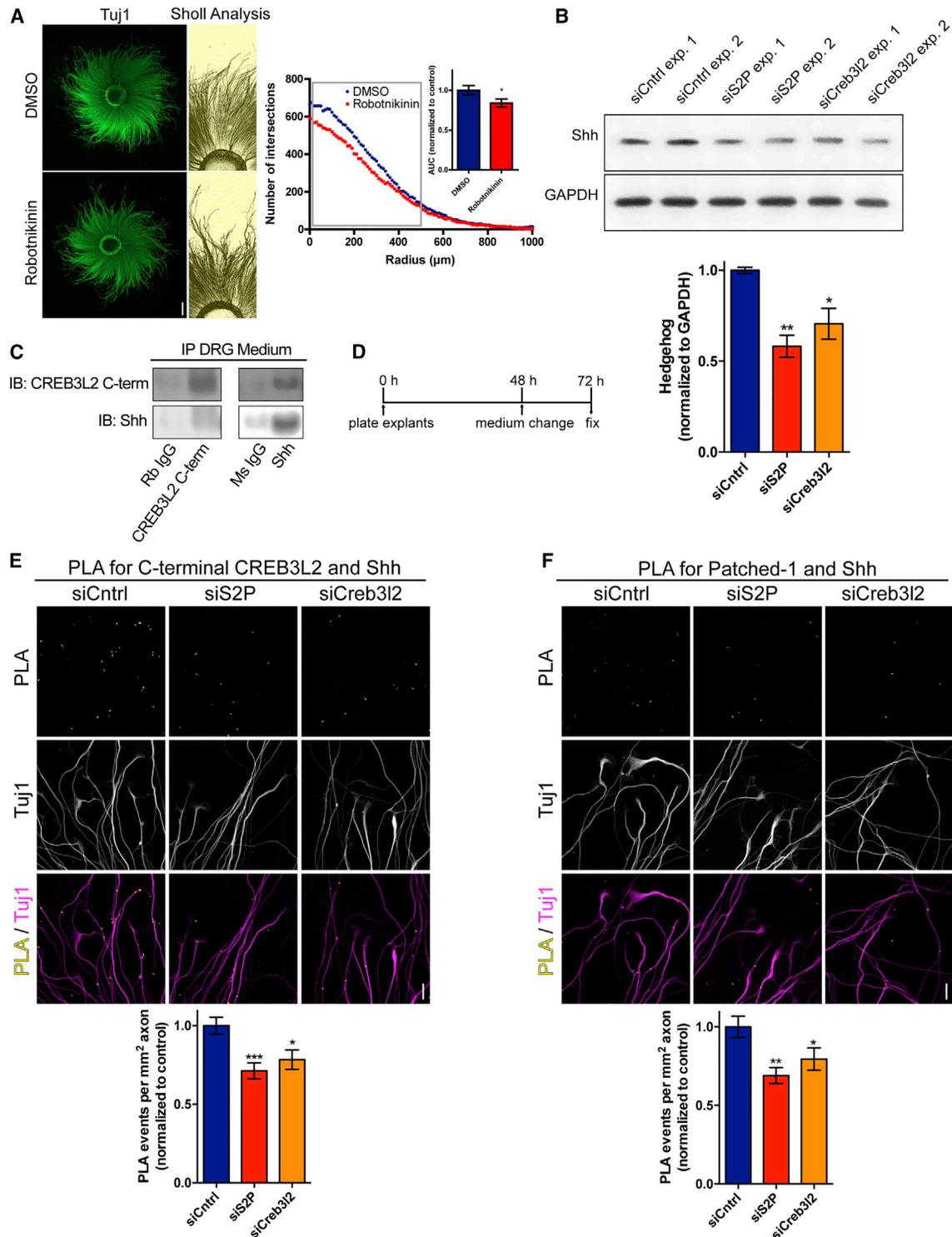
Figure 6. C-Terminal CREB3L2 Promotes Formation of Hh-Patched-1 Complexes in Sensory Axons

(A) DRG explants were cultured for 2 days. On DIV 2, the medium was completely exchanged for DRG growth medium containing 5 ng mL^{-1} NGF and supplemented with either robotnikinin (25 μM) or an equal volume of DMSO for 24 h. On DIV 3, the explants were fixed and visualized for IF by staining against Tuj1, and axon growth was assessed using Sholl analysis. The AUC was measured between conditions. Means ± SEM of 2–3 explants per condition (n = 3 biological replicates). Mann-Whitney t test, *p ≤ 0.05. Scale bar, 250 μm.

(legend continued on next page)

confirmed the specificity of the purified C terminus of CREB3L2 for rescuing axon growth (Figure S3). To determine whether the rescue by C-terminal CREB3L2 was paralleled by restoration of Hh-Patched-1 interactions on axons, we prepared DRG explants electroporated with control or S2P- or CREB3L2-targeting siRNA as before and supplemented the medium with purified C-terminal CREB3L2 (Figure 7D). Although there was a trend toward an increased number of complexes in the siS2P condition compared with control siRNA (siCntrl), no significant differences in the number of PLA puncta were detected between the different conditions, establishing that exogenous C-terminal CREB3L2 is sufficient to restore axon growth (Figure 7C) and rescue the formation of Shh and Patched-1 complexes on DRG axons (Figure 7D).

Overall, our data show that the physiological stress sensor S2P promotes axon growth by cleaving a transcription factor locally, leading to secretion of its luminal domain, which, in turn, promotes the assembly of active Hh signaling machinery on developing sensory axons (Figure 7E). These findings describe a mechanism by which axons can promote their own growth through a cell-autonomous signaling pathway.

DISCUSSION

Axons respond to a repertoire of signaling molecules that control their projection toward target regions. However, the extent to which axons can regulate their own growth is incompletely understood. We discovered that S2P cleaves CREB3L2 in developing DRG axons and that the secreted C terminus promotes axon growth. A question that arises from this finding is why neurons possess a mechanism to modulate growth of their axon through a secreted factor. Current models suggest that adhesive or repellant molecules in the axonal environment or on other neurons create a permissive corridor for axon growth. Mechanisms involving diffusible growth-promoting factors derived from the axon have been suggested, but their necessity remains unresolved. Our results presented here describe a mechanism whereby the secreted portion of a transcription factor creates a local growth-promoting gradient around individual axons that activates Hh signaling. The *in vivo* relevance of this activity remains unknown, but, intriguingly, mutations in the gene encoding S2P cause ichthyosis follicularis, alopecia, and photophobia (IFAP) syndrome, which includes hypoplasia of the *corpus callosum* (Mégarbané and Mégarbané, 2011); i.e., an axon growth phenotype.

We found that the physiological ER stress effectors S2P and CREB3L2 support growth, adding to the emerging realization that low-level ER stress is required for several aspects of neuronal development and function (Cagnetta et al., 2019; Martínez et al., 2016; Wei et al., 2015; Ying et al., 2015). What happens to this signaling pathway in mature neurons? Post-developmental DRGs continue to produce Hh (Brownell et al., 2011), indicating that regulation of S2P downstream of ER stress might be a switch to lower C-terminal CREB3L2 levels to control intra-axonal Hh signaling. In fact, axonal ER stress is positively correlated with axon growth and regeneration (Hayashi et al., 2007; Ohtake et al., 2018; Oñate et al., 2016; Ying et al., 2014).

Although primary DRG cultures were the source for Shh in our study, it is known that, during development and as adult neurons, DRGs encounter additional sources of Hh; for example, Schwann cells, which myelinate DRGs, produce Desert Hh (Parmantier et al., 1999), and Hh signaling in Schwann cells regulates myelination of DRG axons (Yoshimura and Takeda, 2012), raising the possibility that axon-derived C-terminal CREB3L2 facilitates myelination in a paracrine manner. Similarly, adult DRGs supply Hh to bulge cells in the hair follicle to maintain an active stem cell population (Brownell et al., 2011). One possibility is that axon-derived C-terminal CREB3L2 helps modulate the crosstalk between competing sources of Hh protein in these contexts.

An interesting aspect of our findings is that S2P cleavage of CREB3L2 simultaneously generates a transcription factor and a secreted protein that supports axon growth. Whether and how these two signaling modalities are integrated in the control of axon development remains unknown. The fact that we did not detect a requirement for the transcriptional activity of CREB3L2 in our assays is potentially a reflection of the short experimental periods of S2P or CREB3L2 KD, which do not allow for transcriptional deficits to significantly affect axon growth. Among the transcriptional targets of CREB3L2 are genes necessary for coat protein complex II (COPII) vesicle formation, including Sec23a and Sec23b (Melville et al., 2011; Saito et al., 2009). ER exit sites (ERESs), of which Sec23 is a component, are selectively targeted to rapidly growing axons to meet their biosynthetic demands (Aridor and Fish, 2009), indicating that S2P-dependent cleavage of CREB3L2 supports axonal development through secreted C-terminal CREB3L2, which has immediate local effects, and through liberation of the transcription factor, which induces slower transcriptional changes.

In conclusion, our results reveal a neuron-intrinsic mechanism for how developing axons regulate their own growth. We show that S2P-dependent generation of the secreted C terminus of CREB3L2 is required for axon growth, and we identify the S2P-CREB3L2-Shh signaling pathway in developing DRG axons.
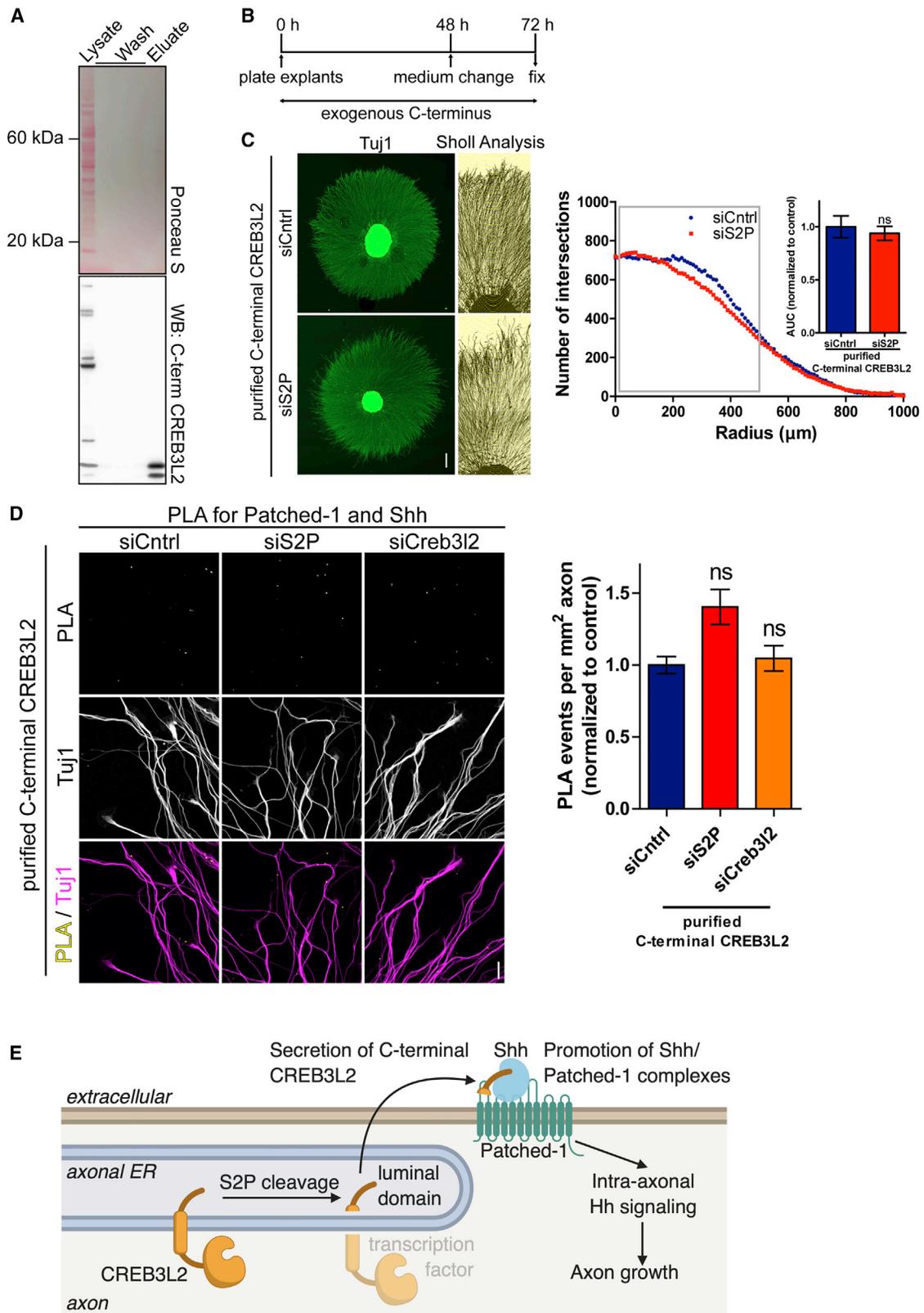

(B) Dissociated DRGs were cultured for 2 DIV and transfected with non-targeting control siRNA or siRNA targeting S2P or CREB3L2 for 72 h. On DIV 5, whole-cell lysates were collected and analyzed by western blot for endogenous Shh. A blot with 2 repeats is shown. Means ± SEM of 4 biological replicates. Kruskal-Wallis test with Dunn's multiple comparisons test, *p ≤ 0.05, **p ≤ 0.01.

(C) Dissociated DRGs were cultured for 2 DIV, and their medium was completely exchanged for DRG growth medium containing 5 ng mL^{-1} NGF for 48 h. The medium was collected on DIV 4, and co-IPs were performed for C-terminal CREB3L2 and Shh.

(D) Experimental design for (E) and (F). DRG explants were electroporated with non-targeting control siRNA or siRNA targeting S2P or CREB3L2. On DIV 2, the medium was completely exchanged for DRG growth medium containing 5 ng mL^{-1} NGF for 24 h. On DIV 3, the explants were fixed and prepared for PLA.

(E and F) DRG explants were fixed and prepared for PLA using antibodies against C-terminal CREB3L2 and Shh (E) or Patched-1 and Shh (F). Means ± SEM of 10–20 optical fields per condition (n = 3 biological replicates). Kruskal-Wallis tests with Dunn's multiple comparisons tests, *p ≤ 0.05, **p ≤ 0.01, ***p ≤ 0.001. Scale bars, 20 μm.

See also Figure S2.

A

Ponceau S

WB: C-term CREB3L2

B

plate explants — medium change — fix

exogenous C-terminus

C

Tuj1   Sholl Analysis

purified C-terminal CREB3L2

siCntrl

siS2P

D

PLA for Patched-1 and Shh

siCntrl   siS2P   siCreb3l2

purified C-terminal CREB3L2

PLA

Tuj1

PLA / Tuj1

E

Secretion of C-terminal CREB3L2   Shh   Promotion of Shh/Patched-1 complexes

extracellular

axonal ER   S2P cleavage   luminal domain   Patched-1

CREB3L2   transcription factor   Intra-axonal Hh signaling

axon   Axon growth

(legend on next page)

STAR★METHODS

Detailed methods are provided in the online version of this paper and include the following:

- KEY RESOURCES TABLE
- LEAD CONTACT AND MATERIALS AVAILABILITY
- EXPERIMENTAL MODEL AND SUBJECT DETAILS
  - DRG Culture
  - HEK293T
- METHOD DETAILS
  - Microfluidic Devices
  - siRNA Transfection and Electroporation
  - Proximity Ligation Assay
  - Quantitative Immunofluorescence
  - Immunohistochemistry
  - Sholl Analysis
  - Live Imaging of DRG Outgrowth
  - DNA Constructs
  - Immunoblot
  - Real-Time RT-PCR
  - Purification of C-terminal CREB3L2
- QUANTIFICATION AND STATISTICAL ANALYSIS
- DATA AND CODE AVAILABILITY

SUPPLEMENTAL INFORMATION

Supplemental Information can be found online at https://doi.org/10.1016/j.celrep.2019.08.101.

AUTHOR CONTRIBUTIONS

E.P.M., with K.M.C. and C.R.B.-A., performed and analyzed all experiments. U.H. conceived the project, and U.H. and E.P.M. designed the experiments and wrote the manuscript.

DECLARATION OF INTERESTS

The authors declare no competing interests.

REFERENCES

Aridor, M., and Fish, K.N. (2009). Selective targeting of ER exit sites supports axon development. Traffic 10, 1669–1684.

Asada, R., Kanemoto, S., Kondo, S., Saito, A., and Imaizumi, K. (2011). The signalling from endoplasmic reticulum-resident bZIP transcription factors involved in diverse cellular physiology. J. Biochem. 149, 507–518.

Baleriola, J., Walker, C.A., Jean, Y.Y., Crary, J.F., Troy, C.M., Nagy, P.L., and Hengst, U. (2014). Axonally synthesized ATF4 transmits a neurodegenerative signal across brain regions. Cell 158, 1159–1172.

Ben-Yaakov, K., Dagan, S.Y., Segal-Ruder, Y., Shalem, O., Vuppalanchi, D., Willis, D.E., Yudin, D., Rishal, I., Rother, F., Bader, M., et al. (2012). Axonal transcription factors signal retrogradely in lesioned peripheral nerve. EMBO J. 31, 1350–1363.

Brown, M.S., and Goldstein, J.L. (1997). The SREBP pathway: regulation of cholesterol metabolism by proteolysis of a membrane-bound transcription factor. Cell 89, 331–340.

Brownell, I., Guevara, E., Bai, C.B., Loomis, C.A., and Joyner, A.L. (2011). Nerve-derived sonic hedgehog defines a niche for hair follicle stem cells capable of becoming epidermal stem cells. Cell Stem Cell 8, 552–565.

Butler, S.J., and Tear, G. (2007). Getting axons onto the right path: the role of transcription factors in axon guidance. Development 134, 439–448.

Cagnetta, R., Wong, H.H., Frese, C.K., Mallucci, G.R., Krijgsveld, J., and Holt, C.E. (2019). Noncanonical Modulation of the eIF2 Pathway Controls an Increase in Local Translation during Neural Wiring. Mol. Cell 73, 474–489.e5.

Charron, F., Stein, E., Jeong, J., McMahon, A.P., and Tessier-Lavigne, M. (2003). The morphogen sonic hedgehog is an axonal chemoattractant that collaborates with netrin-1 in midline axon guidance. Cell 113, 11–23.

Cox, L.J., Hengst, U., Gurskaya, N.G., Lukyanov, K.A., and Jaffrey, S.R. (2008). Intra-axonal translation and retrograde trafficking of CREB promotes neuronal survival. Nat. Cell Biol. 10, 149–159.

Ferreira, T.A., Blackman, A.V., Oyrer, J., Jayabal, S., Chung, A.J., Watt, A.J., Sjöström, P.J., and van Meyel, D.J. (2014). Neuronal morphometry directly from bitmap images. Nat. Methods 11, 982–984.

Firestone, A.J., Weinger, J.S., Maldonado, M., Barlan, K., Langston, L.D., O'Donnell, M., Gelfand, V.I., Kapoor, T.M., and Chen, J.K. (2012).

Figure 7. C-Terminal CREB3L2 Rescues DRG Growth through a Hh-Dependent Mechanism

(A) His-tagged C-terminal CREB3L2 was expressed in HEK293 cells and batch purified using Ni^{2+}-nitrilotriacetic acid (Ni-NTA) resin. Samples of the cell lysates, wash fractions, and the eluate were analyzed by immunoblotting. Images of the Ponceau S-stained membrane and the immunoblot with C-terminal CREB3L2 antibody are shown.

(B) Experimental design for (C). DRG explants were electroporated with non-targeting control siRNA or siRNA targeting S2P and cultured for 2 DIV in medium containing 100 ng mL^{-1} purified C-terminal CREB3L2. On DIV 2, the explant medium was exchanged for fresh medium supplemented with 100 ng mL^{-1} purified C-terminal CREB3L2.

(C) DRG explants were fixed on DIV 3, and axon growth was assessed by Sholl analysis. AUC was measured between conditions. Means ± SEM of 2–5 explants per condition (n = 4 biological replicates). Mann-Whitney t test, ns, not significant. Scale bar, 250 μm.

(D) DRG explants were electroporated with non-targeting control siRNA or siRNA targeting S2P or CREB3L2 and treated with exogenous C-terminal CREB3L2 as described in (B). The explants were then fixed and prepared for PLA using antibodies against Hh and Patched-1. Means ± SEM of 4 biological replicates. Kruskal-Wallis tests with Dunn's multiple comparisons tests, ns, not significant. Scale bar, 20 μm.

(E) Model of the proposed mechanism for regulation of axon growth by C-terminal CREB3L2. CREB3L2 is cleaved in developing DRG axons by S2P, and the C terminus is secreted. C-terminal CREB3L2 binds Hh and promotes its association with the Patched-1 receptor. Activation of intracellular Hh signaling promotes axon growth in a neuron-intrinsic manner.

See also Figure S3.

Small-molecule inhibitors of the AAA+ ATPase motor cytoplasmic dynein. Nature 484, 125–129.

González, C., Cánovas, J., Fresno, J., Couve, E., Court, F.A., and Couve, A. (2016). Axons provide the secretory machinery for trafficking of voltage-gated sodium channels in peripheral nerve. Proc. Natl. Acad. Sci. USA 113, 1823–1828.

Guan, M., Fousek, K., Jiang, C., Guo, S., Synold, T., Xi, B., Shih, C.C., and Chow, W.A. (2011). Nelfinavir induces liposarcoma apoptosis through inhibition of regulated intramembrane proteolysis of SREBP-1 and ATF6. Clin. Cancer Res. 17, 1796–1806.

Guan, M., Fousek, K., and Chow, W.A. (2012). Nelfinavir inhibits regulated intramembrane proteolysis of sterol regulatory element binding protein-1 and activating transcription factor 6 in castration-resistant prostate cancer. FEBS J. 279, 2399–2411.

Guan, M., Su, L., Yuan, Y.C., Li, H., and Chow, W.A. (2015). Nelfinavir and nelfinavir analogs block site-2 protease cleavage to inhibit castration-resistant prostate cancer. Sci. Rep. 5, 9698.

Hayashi, A., Kasahara, T., Iwamoto, K., Ishiwata, M., Kametani, M., Kakiuchi, C., Furuichi, T., and Kato, T. (2007). The role of brain-derived neurotrophic factor (BDNF)-induced XBP1 splicing during brain development. J. Biol. Chem. 282, 34525–34534.

Hengst, U., Deglincerti, A., Kim, H.J., Jeon, N.L., and Jaffrey, S.R. (2009). Axonal elongation triggered by stimulus-induced local translation of a polarity complex protein. Nat. Cell Biol. 11, 1024–1030.

Hoppe, T., Rape, M., and Jentsch, S. (2001). Membrane-bound transcription factors: regulated release by RIP or RUP. Curr. Opin. Cell Biol. 13, 344–348.

Horton, J.D., Shah, N.A., Warrington, J.A., Anderson, N.N., Park, S.W., Brown, M.S., and Goldstein, J.L. (2003). Combined analysis of oligonucleotide microarray data from transgenic and knockout mice identifies direct SREBP target genes. Proc. Natl. Acad. Sci. USA 100, 12027–12032.

Ji, S.J., and Jaffrey, S.R. (2012). Intra-axonal translation of SMAD1/5/8 mediates retrograde regulation of trigeminal ganglia subtype specification. Neuron 74, 95–107.

Kondo, S., Saito, A., Hino, S., Murakami, T., Ogata, M., Kanemoto, S., Nara, S., Yamashita, A., Yoshinaga, K., Hara, H., and Imaizumi, K. (2007). BBF2H7, a novel transmembrane bZIP transcription factor, is a new type of endoplasmic reticulum stress transducer. Mol. Cell. Biol. 27, 1716–1729.

Kondo, S., Saito, A., Asada, R., Kanemoto, S., and Imaizumi, K. (2011). Physiological unfolded protein response regulated by OASIS family members, transmembrane bZIP transcription factors. IUBMB Life 63, 233–239.

Lepelletier, L., Langlois, S.D., Kent, C.B., Welshhans, K., Morin, S., Bassell, G.J., Yam, P.T., and Charron, F. (2017). Sonic Hedgehog Guides Axons via Zipcode Binding Protein 1-Mediated Local Translation. J. Neurosci. 37, 1685–1695.

Longair, M.H., Baker, D.A., and Armstrong, J.D. (2011). Simple Neurite Tracer: open source software for reconstruction, visualization and analysis of neuronal processes. Bioinformatics 27, 2453–2454.

Martinez, J.A., Kobayashi, M., Krishnan, A., Webber, C., Christie, K., Guo, G., Singh, V., and Zochodne, D.W. (2015). Intrinsic facilitation of adult peripheral nerve regeneration by the Sonic hedgehog morphogen. Exp. Neurol. 271, 493–505.

Martínez, G., Vidal, R.L., Mardones, P., Serrano, F.G., Ardiles, A.O., Wirth, C., Valdés, P., Thielen, P., Schneider, B.L., Kerr, B., et al. (2016). Regulation of Memory Formation by the Transcription Factor XBP1. Cell Rep. 14, 1382–1394.

Mégarbané, H., and Mégarbané, A. (2011). Ichthyosis follicularis, alopecia, and photophobia (IFAP) syndrome. Orphanet J. Rare Dis. 6, 29.

Melville, D.B., Montero-Balaguer, M., Levic, D.S., Bradley, K., Smith, J.R., Hatzopoulos, A.K., and Knapik, E.W. (2011). The feelgood mutation in zebrafish dysregulates COPII-dependent secretion of select extracellular matrix proteins in skeletal morphogenesis. Dis. Model. Mech. 4, 763–776.

Merianda, T., and Twiss, J. (2013). Peripheral nerve axons contain machinery for co-translational secretion of axonally-generated proteins. Neurosci. Bull. 29, 493–500.

Merianda, T.T., Lin, A.C., Lam, J.S., Vuppalanchi, D., Willis, D.E., Karin, N., Holt, C.E., and Twiss, J.L. (2009). A functional equivalent of endoplasmic reticulum and Golgi in axons for secretion of locally synthesized proteins. Mol. Cell. Neurosci. 40, 128–142.

Ohtake, Y., Matsuhisa, K., Kaneko, M., Kanemoto, S., Asada, R., Imaizumi, K., and Saito, A. (2018). Axonal Activation of the Unfolded Protein Response Promotes Axonal Regeneration Following Peripheral Nerve Injury. Neuroscience 375, 34–48.

Okada, A., Charron, F., Morin, S., Shin, D.S., Wong, K., Fabre, P.J., Tessier-Lavigne, M., and McConnell, S.K. (2006). Boc is a receptor for sonic hedgehog in the guidance of commissural axons. Nature 444, 369–373.

Oñate, M., Catenaccio, A., Martínez, G., Armentano, D., Parsons, G., Kerr, B., Hetz, C., and Court, F.A. (2016). Activation of the unfolded protein response promotes axonal regeneration after peripheral nerve injury. Sci. Rep. 6, 21709.

Park, J.W., Vahidi, B., Taylor, A.M., Rhee, S.W., and Jeon, N.L. (2006). Microfluidic culture platform for neuroscience research. Nat. Protoc. 1, 2128–2136.

Parmantier, E., Lynn, B., Lawson, D., Turmaine, M., Namini, S.S., Chakrabarti, L., McMahon, A.P., Jessen, K.R., and Mirsky, R. (1999). Schwann cell-derived Desert hedgehog controls the development of peripheral nerve sheaths. Neuron 23, 713–724.

Pathi, S., Pagan-Westphal, S., Baker, D.P., Garber, E.A., Rayhorn, P., Bumcrot, D., Tabin, C.J., Blake Pepinsky, R., and Williams, K.P. (2001). Comparative biological responses to human Sonic, Indian, and Desert hedgehog. Mech. Dev. 106, 107–117.

Pfenninger, K.H. (2009). Plasma membrane expansion: a neuron's Herculean task. Nat. Rev. Neurosci. 10, 251–261.

Polleux, F., Ince-Dunn, G., and Ghosh, A. (2007). Transcriptional regulation of vertebrate axon guidance and synapse formation. Nat. Rev. Neurosci. 8, 331–340.

Rawson, R.B. (2013). The site-2 protease. Biochim. Biophys. Acta 1828, 2801–2807.

Saito, A., Hino, S., Murakami, T., Kanemoto, S., Kondo, S., Saitoh, M., Nishimura, R., Yoneda, T., Furuichi, T., Ikegawa, S., et al. (2009). Regulation of endoplasmic reticulum stress response by a BBF2H7-mediated Sec23a pathway is essential for chondrogenesis. Nat. Cell Biol. 11, 1197–1204.

Saito, A., Kanemoto, S., Zhang, Y., Asada, R., Hino, K., and Imaizumi, K. (2014). Chondrocyte proliferation regulated by secreted luminal domain of ER stress transducer BBF2H7/CREB3L2. Mol. Cell 53, 127–139.

Schindelin, J., Arganda-Carreras, I., Frise, E., Kaynig, V., Longair, M., Pietzsch, T., Preibisch, S., Rueden, C., Saalfeld, S., Schmid, B., et al. (2012). Fiji: an open-source platform for biological-image analysis. Nat. Methods 9, 676–682.

Shen, J., and Prywes, R. (2004). Dependence of site-2 protease cleavage of ATF6 on prior site-1 protease digestion is determined by the size of the luminal domain of ATF6. J. Biol. Chem. 279, 43046–43051.

Shen, J., Chen, X., Hendershot, L., and Prywes, R. (2002). ER stress regulation of ATF6 localization by dissociation of BiP/GRP78 binding and unmasking of Golgi localization signals. Dev. Cell 3, 99–111.

Stanton, B.Z., Peng, L.F., Maloof, N., Nakai, K., Wang, X., Duffner, J.L., Taveras, K.M., Hyman, J.M., Lee, S.W., Koehler, A.N., et al. (2009). A small molecule that binds Hedgehog and blocks its signaling in human cells. Nat. Chem. Biol. 5, 154–156.

Stoeckli, E.T. (2018). Understanding axon guidance: are we nearly there yet? Development 145, dev151415.

Taylor, A.M., Blurton-Jones, M., Rhee, S.W., Cribbs, D.H., Cotman, C.W., and Jeon, N.L. (2005). A microfluidic culture platform for CNS axonal injury, regeneration and transport. Nat. Methods 2, 599–605.

Trousse, F., Martí, E., Gruss, P., Torres, M., and Bovolenta, P. (2001). Control of retinal ganglion cell axon growth: a new role for Sonic hedgehog. Development 128, 3927–3936.

Twelvetrees, A.E., Pernigo, S., Sanger, A., Guedes-Dias, P., Schiavo, G., Steiner, R.A., Dodding, M.P., and Holzbaur, E.L. (2016). The Dynamic Localization of Cytoplasmic Dynein in Neurons Is Driven by Kinesin-1. Neuron 90, 1000–1015.

Wei, X., Howell, A.S., Dong, X., Taylor, C.A., Cooper, R.C., Zhang, J., Zou, W., Sherwood, D.R., and Shen, K. (2015). The unfolded protein response is required for dendrite morphogenesis. eLife 4, e06963.

Yam, P.T., Langlois, S.D., Morin, S., and Charron, F. (2009). Sonic hedgehog guides axons through a noncanonical, Src-family-kinase-dependent signaling pathway. Neuron 62, 349–362.

Ying, Z., Misra, V., and Verge, V.M. (2014). Sensing nerve injury at the axonal ER: activated Luman/CREB3 serves as a novel axonally synthesized retrograde regeneration signal. Proc. Natl. Acad. Sci. USA 111, 16142–16147.

Ying, Z., Zhai, R., McLean, N.A., Johnston, J.M., Misra, V., and Verge, V.M. (2015). The Unfolded Protein Response and Cholesterol Biosynthesis Link Luman/CREB3 to Regenerative Axon Growth in Sensory Neurons. J. Neurosci. 35, 14557–14570.

Yoshimura, K., and Takeda, S. (2012). Hedgehog signaling regulates myelination in the peripheral nervous system through primary cilia. Differentiation 83, S78–S85.

STAR★METHODS

KEY RESOURCES TABLE

REAGENT or RESOURCE	SOURCE	IDENTIFIER
Antibodies		
Chicken polyclonal anti-Neurofilament	Abcam	Cat# ab4680; RRID: AB_304560
Rabbit polyclonal anti-S2P	Abcam	Cat# ab196797; RRID: AB_2811284
Mouse monoclonal anti-S2P (1A3)	Santa Cruz	Cat# sc-293341
Rabbit polyclonal anti-CREB3L2 C terminus	Abcam	Cat# ab102989; RRID: AB_10711653
Rabbit polyclonal anti-CREB3L2 N terminus	Atlas Antibodies	Cat# HPA015534; RRID: AB_2669210
Mouse monoclonal anti-CREB3L2 N terminus	Santa Cruz	Cat# sc-515816
Mouse monoclonal 488 anti-βIII-tubulin (clone Tuj1)	Biolegend	Cat# 801203; RRID: AB_2564757
Mouse monoclonal anti-Shh (E-1)	Santa Cruz	Cat# sc-365112; RRID: AB_10709580
Rabbit polyclonal anti-Ptch1	Proteintech	Cat# 17520-1-AP; RRID: AB_2176561
Mouse monoclonal anti-GAPDH (6C5)	Santa Cruz	Cat# sc-32233; RRID: AB_627679
Bacterial and Virus Strains		
Stellar Competent Cells	Takara	Cat# 636766
Chemicals, Peptides, and Recombinant Proteins		
DMSO	Sigma-Aldrich	Cat# D8418
Nelfinavir	Sigma-Aldrich	Cat# CDS021783
Ciliobrevin A	R&D Systems	Cat# 4529
Robotnikinin	Fisher Scientific	Cat# 50464659
Tissue Tek OCT Compound	Fisher Scientific	Cat# 50363579
Critical Commercial Assays		
iTaq Universal Probes One-Step Kit	Bio-Rad	Cat# 172-5140
Duolink *In Situ* Detection Reagents Red	Sigma-Aldrich	Cat# DUO92008
Duolink *In Situ* PLA Probe Anti-Mouse Plus	Sigma-Aldrich	Cat# DUO92001
Duolink *In Situ* PLA Probe Anti-Rabbit Minus	Sigma-Aldrich	Cat# DUO92005
Promega DeadEnd Fluorometric TUNEL System	Fisher Scientific	Cat# PRG3250
Experimental Models: Cell Lines		
Human: HEK293T	ATCC	Cat# CRL-3216
Experimental Models: Organisms/Strains		
Rat: Hsd:Sprague Dawley SD	Envigo	Hsd:Sprague Dawley SD – 002
Oligonucleotides		
Stealth siRNA targeting sequence (S2P, RSS313818)	Thermo Fisher Scientific	Cat# 1330001
Stealth siRNA targeting sequence (CREB3L2, RSS324942)	Thermo Fisher Scientific	Cat# 1330001
Stealth RNAi siRNA Negative Control Med GC Duplex #3	Thermo Fisher Scientific	Cat# 12935113
Mbtps2 (Rn01752838_m1)	Thermo Fisher Scientific	Cat# 4331182
Creb3l2 (Rn01455999_m1)	Thermo Fisher Scientific	Cat# 4331182
Fasn (Rn00569117_m1)	Thermo Fisher Scientific	Cat# 4331182
Hmgcr (Rn00565598_m1)	Thermo Fisher Scientific	Cat# 4331182
Tubb3 (Rn01431594_m1)	Thermo Fisher Scientific	Cat# 4331182
Recombinant DNA		
Plasmid: EX-H2495-M01 (CREB3L2)	Genecopoeia	Cat# H2495
Plasmid: pEGFP-C1 (GFP)	Takara Bio	discontinued
Plasmid: pmCherry-C1 (mCherry)	Takara Bio	Cat# 632524
Plasmid: GCM	This paper	N/A

(Continued on next page)

Continued

REAGENT or RESOURCE	SOURCE	IDENTIFIER
Plasmid: C-terminal CREB3L2	This paper	N/A
Plasmid: pCGN-S2P-WT	Shen et al., 2002	Addgene Cat# 32957, RRID:Addgene_32957
Plasmid: siRNA-resistant S2P	This paper	N/A
Software and Algorithms		
ImageJ (FIJI)	Schindelin et al., 2012	https://imagej.net/Fiji
Sholl analysis	Ferreira et al., 2014	https://imagej.net/Sholl_Analysis
Neurite Tracer	Longair et al., 2011	https://imagej.net/Simple_Neurite_Tracer
Axiovision	Zeiss	N/A
GraphPad Prism 8 (version 8.1.2)	GraphPad	https://www.graphpad.com/scientific-software/prism/
Other		
SYLGARD	Ellsworth Adhesives	Cat# 4019862
4-inch silicon wafers	University Wafer	Cat# 783
SU-8 5	MicroChem Corp.	Cat# Y131252
SU-8 2050	MicroChem Corp.	Cat# Y111072
In-Fusion® HD EcoDry Cloning Plus	Takara Bio	Cat# 638913

LEAD CONTACT AND MATERIALS AVAILABILITY

Further information and requests for resources and reagents should be directed to and will be fulfilled by the Lead Contact, Ulrich Hengst (uh2112@cumc.columbia.edu). Plasmids generated in this study are available on request.

EXPERIMENTAL MODEL AND SUBJECT DETAILS

DRG Culture

All work involving animals was performed according to the NIH guidelines for the care and use of laboratory animals and was approved by the Institutional Animal Use and Care Committee (IACUC) of Columbia University. All reagents were purchased from Thermo Fisher Scientific unless otherwise noted. DRG neurons were harvested from Sprague-Dawley embryonic day 14 rat embryos of both sexes. Explants were harvested by individually removing clusters of ganglia from similar areas across conditions. For compartmentalized and dissociated cultures, DRG explants were dissociated in TrypLE and seeded (30,000 per compartmentalized chamber or 400,000 per well in 6-well plates) in plating medium (Neurobasal, 1 X B27, 1 X Pen/Strep, 100 mM glutamine, 25 μM 5′-fluorodeoxyuridine, 50 ng ml^{-1} NGF). NGF was purchased from R&D Systems (256-GF-100/CF). The plating medium was entirely exchanged after 48 h for growth medium (Neurobasal, 1 X B27, 100 mM glutamine, 5 ng ml^{-1} NGF) in all wells or compartments. Devices were composed of three compartments (width of middle axonal compartment: 500 μm; somatic and distal axonal compartments: 1,500 μm) connected by two microgroove barriers (microgroove length: 500 μm, width 10 μm, height: 3 μm). Prior to plating cells, 100 μg ml^{-1} poly-L-lysine (Trevigen, Gaithersburg, MD) was used to coat all coverslips or dishes. For explants only, PLL coating was followed by a 2 h coating with 1 μg ml^{-1} laminin (Trevigen) in growth medium. For live-imaging and PLA assays, DRG cultures were prepared on glass bottom cultures dishes (MatTek, Ashland, MA) and coated as described above.

HEK293T

HEK293T cells, a human embryonic kidney derived cell line expressing a mutant form of the SV40 large T antigen, were cultured in DMEM medium supplemented with 10% fetal bovine serum (Thermo Fisher Scientific, Waltham, MA) in a humified atmosphere of 5% CO_2 at 37°C. HEK293T cells were grown to 50%–70% confluency before transfection.

METHOD DETAILS

Microfluidic Devices

Tripartite microfluidic devices were produced from molds designed in-house and manufactured at the Advanced Science Research Center NanoFabrication Facility of the Graduate Center at the City University of New York, based on previous reports (Park et al., 2006; Taylor et al., 2005). Briefly, photomasks were designed using AutoCAD software and ordered according to specification (Front Range Photomask). To manufacture the microfluidic silicon masters, 100 mm silicon wafers (University Wafer, Inc.) were dehydrated at 200°C for 5 minutes and cleaned with pressurized nitrogen. The grooves of the microfluidics were produced by spinning a layer of SU-8 at 2500 rpm for 60 s, aligning the wafer to the photomask containing the grooves, and exposing the SU-8 layer to 100 mJ/cm^2

UV using a Nanoscribe Photonic Professional 3D Lithography mask aligner. The wafer was then hard-baked at 95°C and developed in propylene glycol methyl ether acetate (SU-8 developer). The wells of the microfluidics were produced by spinning a layer of SU-8 2050 over the groove layer at 1500 rpm for 60 s. The photomask for the wells was then aligned over the existing layer of microgrooves on the wafer using the mask aligner and exposed to 230 mJ/cm^2 UV. Afterward, the wafer was hard-baked at 95°C and submerged in SU-8 developer, cleaned with isopropanol, and hard-baked for 10 m at 150°C.

After the masters were manufactured, the tripartite microfluidic devices were produced from a 9:1 elastomer base to curing agent mixture of Sylgard 184 (Ellsworth Adhesives). Individual microfluidic chambers were cut out and the reservoirs were opened with a sterile biopsy punch. The chambers were then cleaned with vinyl tape and washed briefly in 70% ethanol in a cell culture hood and allowed to air-dry before use.

siRNA Transfection and Electroporation

Silencing of *Mbtps2* and *Creb3l2* mRNAs in microfluidic devices was achieved by transfecting siRNAs together with the medium change on DIV2 using NeuroPORTER (Genlantis, San Diego, CA) as the transfection reagent. The silencing of these transcripts in dissociated DRGs was achieved using the siRNA transfection guidelines of Lipofectamine 3000 transfection reagent (Thermo Fisher Scientific). For outgrowth assays, all transfections were performed on DIV2 for 48 h in growth medium. Electroporation of siRNA into DRG explants was achieved as follows: whole-strip DRG explants were stuck in place to the bottom of a 0.4 cm Gene Pulser cuvette (Bio-Rad, Hercules, CA). Electroporations were carried out in 1X MMR buffer (100 mM NaCl, 2 mM KCl, 1 mM MgSO$_4$, 2 mM CaCl$_2$, 5 mM HEPES, 1 mM EDTA) using a ECM830 Square Wave Porator Harvard Apparatus (BTX, Holliston, MA) with the following program: 100 V, 50 ms pulse length, 4 pulses, 1 s interval. Explants were transferred to cold Leibovitz's L-15 medium immediately following electroporation. Electroporations of siCntrl, siS2P, and siCreb3l2 used for Sholl analyses were all performed in parallel. The following siRNAs were used to target rat *Mbtps2* (NM_001035007.1): 5′-GCAUACAUGUCUACCUGCCCGGAAA-3′ and 5′-UUUCCGGGCAGGUAGACAUGUAUGC-3′; and *Creb3l2* (NM_001012188.1): 5′-CGAGGGCUAUCCCAUUCCAACCAAA-3′ and 5′-UUUGGUUGGAAUGGGAUAGCCCUCG-3′. Negative control siRNA was purchased from ThermoFisher Scientific (Stealth RNAi siRNA Negative Control Med GC Duplex #3). The efficacy of each siRNA was validated by RT-PCR.

Proximity Ligation Assay

To detect protein-protein complexes in compartmentalized or explant cultures, DRGs were fixed for 20 min at room temperature in 4% PFA in cytoskeletal buffer (10 mM 2-(N-morpholino)ethanesulfonic acid [MES], 3 mM MgCl$_2$, 138 mM KCl, 2 mM EGTA, 0.32 M sucrose [pH 6.1]). DRGs were washed with TBS, permeabilized, and blocked for 30 min with 3 mg ml^{-1} BSA, 100 mM glycine, and 0.25% Triton X-100. Coverslips were incubated overnight at 4°C with primary antibodies: mouse N-terminal CREB3L2 (1:100, Santa Cruz, 515816), rabbit C-terminal CREB3L2 (1:100, abcam, 102989), mouse Hedgehog (1:100, Santa Cruz, 365112), rabbit Patched-1 (1:100, ProteinTech, 17520-1-AP). Detection of PLA complexes was performed according to the manufacturer recommendations, using mouse PLA^{plus} and rabbit PLA^{minus} probes and red Duolink detection reagents (Sigma-Aldrich). Following PLA, tubulin was labeled with anti-βIII-tubulin conjugated to Alexa Fluor 488 (1:500, BioLegend, 801203). Images were acquired using a Zeiss LSM 800 confocal microscope using a 40x oil objective and Zen Blue 2.1 software. Positive PLA puncta were counted and normalized to the area of tubulin-labeled axons.

Quantitative Immunofluorescence

DRGs were cultured as described above and fixed for 20 min at room temperature in 4% PFA in cytoskeletal buffer (10 mM 2-(N-morpholino)ethanesulfonic acid [MES], 3 mM MgCl$_2$, 138 mM KCl, 2 mM EGTA, 0.32 M sucrose [pH 6.1]). DRGs were washed with TBS, permeabilized, and blocked for 30 min with 3 mg ml^{-1} BSA, 100 mM glycine, and 0.25% Triton X-100. Coverslips or optical dishes were incubated overnight at 4°C with primary antibodies: rabbit S2P (1:200, Abcam, 196797), mouse S2P (1:100, Santa Cruz, 293341), rabbit N-terminal CREB3L2 (1:100, Sigma-Aldrich, HPA015534), rabbit C-terminal CREB3L2 (1:100, Abcam, 102989). DRGs were washed with TBS and incubated with fluorophore-conjugated Alexa secondary antibodies (1:500) and anti-βIII-tubulin conjugated to Alexa Fluor 488 (1:500, BioLegend, 801203) in the dark for 1 h at room temperature. Samples were mounted with ProLong Diamond Antifade (Invitrogen, Carlsbad, CA) and images were acquired in z stacks using a 63x/1.3 oil objective on an Axio Observer.Z1 inverted microscope equipped with an AxioCam MRm Rev 3. Camera (Zeiss, Thornwood, NY). All acquisition settings were kept the same for each set of samples in any given experiment. For detection of secreted CREB3L2 only, DRGs were not permeabilized before labeling with the C-terminal antibody. Following incubation with C-terminal CREB3L2 overnight at 4 degrees in a BSA/TBS buffer, DRGs were permeabilized and labeled with fluorophore-conjugated Alexa secondaries and conjugated tubulin following three washes with TBS to remove any excess, unbound C-terminal CREB3L2 antibody.

Immunohistochemistry

To prepare the *in vivo* spinal cord and DRG section, a small (4 mm) midline portion of an E16 rat embryo was isolated in a 10 cm dish of cold HBSS. The blood was cleared with two brief washes in 50 mL cold HBSS. The section was then fixed with 20 mL of 4% PFA in cytoskeletal buffer (10 mM 2-(N-morpholino)ethanesulfonic acid [MES], 3 mM MgCl$_2$, 138 mM KCl, 2 mM EGTA, 0.32 M sucrose [pH 6.1]) for 3 hours (penetrance is approximately 2 to 3 mm per hour). The PFA was removed with 2 washes in TBS and was followed by sucrose infiltration at 10%, 20%, and 30% in TBS until the sample reached the bottom of the vial in each solution. The sample was

then embedded in O.C.T compound (Fisher Scientific) on dry ice. 20 μm sections were taken from the O.C.T. block with a Microm HM505e cryostat, and inverted onto Superfrost Plus coverglass (Fisher Scientific). The sections were permeabilized in TBS containing 0.1% Tween-20 and blocked for 30 min with 3 mg ml^{-1} BSA, 100 mM glycine, and 0.25% Triton X-100 for 30 minutes. Afterward, the sections were incubated overnight at 4°C with rabbit S2P (1:100, Abcam, 196797) and chicken Neurofilament (1:500, Abcam, 4680) primary antibodies in BGT. The following day the sections were washed with TBS and incubated with fluorophore-conjugated Alexa secondary antibodies (1:500) in the dark for 1 h at room temperature. Samples were mounted with ProLong Diamond Antifade (Invitrogen, Carlsbad, CA) and images were acquired using a Zeiss LSM 800 confocal microscope using a 10x objective and 40x oil objective and Zen Blue 2.1 software.

Sholl Analysis

Growth of axons from DRG explants was quantified using the Sholl analysis FIJI plugin (Ferreira et al., 2014). Briefly, explant images were imported into FIJI and thresholded to comparable levels across conditions. A straight line was drawn from the center of the ganglia to the most distal axonal region to establish the center of analysis, or starting radius, and the ending radius. The radius step size was defined as 10 μm. The output of this analysis gave the number of axonal intersections (axons encountered in any given shell) per radius, giving the resulting plot for number of intersections over 2D distance in micrometers. Because the ganglia or cell bodies are also measured in this approach, the total number of concentric circles were divided, and the second half of the circles were analyzed in order to restrict the analysis to axons only. To plot the Sholl analysis, the average number of intersections per radii were plotted along every 10 μm radius for each condition. The area under curve (AUC) was calculated for each explant per condition to determine changes in axon growth.

Live Imaging of DRG Outgrowth

Outgrowth of DRG axons was visualized using an Axio Observer.Z1 inverted microscope equipped with an AxioCam MRm Rev 3. Camera (Zeiss, Thornwood, NY). DRGs were seeded in microfluidic devices as described above and all outgrowth assays were performed on DIV4. During imaging, neurons were kept in a CO$_2$- and humidity-controlled incubation chamber maintained at 37°C. At the beginning of each outgrowth assay, initial images of groups of individual axons were acquired along the second set of microgrooves distal to the cell body ($\geq$ 1,500 μm from soma to growth cone) for t = 0 h. Fresh growth medium containing 5 ng ml^{-1} NGF was applied to the axonal compartment and axons were allowed to grow for 1 h. When used, nelfinavir (Sigma-Aldrich) was supplemented in the fresh growth medium at a final concentration of 15 μM. Images were acquired from the same fields imaged at t = 0 h and the average rate of growth was calculated for every axon as the distance spanned between t = 0 h and t = 1 h using the FIJI plugin Simple Neurite Tracer (Longair et al., 2011). Only axons that grew individually (that is did not make contact with another axon during the assay) were counted. Any minor retractions in growth were scored as zero.

DNA Constructs

The GFP-CREB3L2-mCherry (GCM) construct was produced by modifying a full-length CREB3L2 plasmid that was originally obtained from Genecopoeia (EX-H2495-M01-GS; NM_194071). First, the open reading frame (ORF) of CREB3L2 was subcloned into a vector containing GFP (Takara, pEGFP-C1) using the In Fusion HD Cloning Plus kit (Takara, 638913). Afterward, the ORF for mCherry (Takara, pmCherry-C1, 632524) was amplified and inserted into the GFP-CREB3L2 construct using the In Fusion kit. To produce the C-terminal fragment of CREB3L2 used for purification, the full-length CREB3L2 plasmid was modified by site-directed mutagenesis using the In Fusion kit to produce an ORF encoding a start codon followed by the truncated human protein that results from the cleavage site of S2P, which contains amino acids 386 through 520, followed by a hexa-histidine tag. The CREB3L2 constructs were cloned using Stellar competent cells (Takara, 636766) and purified with the ZymoPure Plasmid Midiprep kit (Zymo Research). The S2P construct pCGN-S2P-WT was a gift from Ron Prywes (Addgene, 32957). The siRNA-resistant S2P construct was created by introducing silent mutations in the sequence recognized by the stealth siRNA targeting S2P. The sequences of all DNA products described above were validated by Sanger sequencing.

Immunoblot

DRGs were cultured in 6-well plates at a density of 400,000 cells per well. For protein isolation, each well was washed once in cold HBSS and collected in 100 μL cold RIPA buffer supplemented with protease and phosphatase inhibitors (Pierce). For HEK293T cells, lysates were collected 24 h after transfection with a fusion CREB3L2 construct (GFP-CREB3L2-mCherry or GFP-CREB3L2-FLAG) ± S2P in 500 μL cold RIPA. Samples were rotated for 30 m at 4°C followed by centrifugation at 12,000 rpm for 20 m at 4°C. 10 μL of supernatant was mixed 1:1 with 10 μL 2X Laemmli sample buffer (4% SDS, 20% glycerol, 120 mM Tris-HCl [pH 6.8]) containing 10% β-mercaptoethanol, and heated at 100°C for 5 m to be used for immunoblot. Following transfer, PVDF membranes were incubated with the antibody of interest at 4°C overnight in BSA or milk in TBS-T. For detection, blots were washed in TBS-T and incubated with their respective secondary antibodies (1:5,000 anti-Ms-HRP or anti-Rb-HRP) for 1 h at room temperature and developed with 1-Shot Digital-ECL (KindleBio, R1003). For immunoprecipitation only, veriblot (Abcam, 131366) was used as the detection reagent. Immunoprecipitation of C-terminal CREB3L2 from DRG medium was performed according to Abcam's technical manual for IP. In summary, dissociated rat DRGs were cultured *in vitro* as described earlier and the medium covering the cells was collected. The medium was centrifuged 10,000 g for 20 minutes at 4°C to remove any debris. Afterward the media was collected and supplemented with

1:500 protease and phosphatase inhibitors (Pierce) and incubated overnight with a primary antibody against either Shh or the C terminus of CREB3L2, or the appropriate control IgG antibody species. The following day, BSA-blocked magnetic Dynabeads that recognized the correct antibody species were added to the DRG medium containing the primary antibody and rotated overnight at 4°C. The following day, the beads were pulled down with a magnet on ice. The samples were washed 4-5 times with cold wash buffer (10 mM Tris-HCl [pH 7.4], 150 mM NaCl, 0.1% Tween-20). Samples were prepared for Western as described above. Images for all immunoblots were acquired using the KwikQuant Imager (KindleBio, D1001).

Real-Time RT-PCR

Total RNA from explants (4-5 explants per condition) was collected 72 h after plating and extracted with RNA lysis buffer, followed by RNA purification using the Direct-zol RNA MicroPrep kit (Zymo Research, Irvine, CA). RNA was reverse-transcribed and amplified using the iTaq Universal Probes 1-Step kit (Bio-Rad, Hercules, CA) in a StepOnePlus Real-Time PCR instrument, using pre-designed Taqman probes. Amplification conditions were the following: reverse transcription for 10 min at 50°C, initial denaturation for 3 m at 95°C, and 40 cycles of denaturation for 15 s at 95°C followed by extension for 1 m at 60°C. Target transcripts were normalized to *Tubb3*.

Purification of C-terminal CREB3L2

HEK293 cells were cultured to approximately 50% confluency and transfected for 24 h with a plasmid encoding C-terminal CREB3L2 followed by a hexa-histidine tag. Cells were lysed in cold RIPA buffer supplemented with protease and phosphatase inhibitors (Pierce). The lysate was collected on ice and passed through a 21G1 needle followed by a 25G5/8 needle three to five times to shear DNA. The lysates were centrifuged at 4°C for 20 minutes at 12,000 rpm and the supernatant containing C-terminal CREB3L2 was collected. The C terminus was purified using HisPur Ni-NTA resin (Thermo) according to the manufacturer instructions for purification of His-tagged proteins by batch method. The final elution was desalted using an Amicon Ultracel-3K centrifugal filter unit (Millipore) and the purified product was measured by BCA analysis (Pierce) and confirmed by Western.

QUANTIFICATION AND STATISTICAL ANALYSIS

All experiments were performed in at least three biological replicates. Two means were compared by two-tailed Mann-Whitney unpaired t tests, whereas multiple means were compared by Kruskal-Wallis tests with Dunn's multiple comparisons tests. Statistical analysis was performed using Prism 6 (GraphPad).

DATA AND CODE AVAILABILITY

This study did not generate datasets.